2018

Retinoid isomerase inhibitors impair but do not block mammalian cone photoreceptor function

Philip D. Kiser
Case Western Reserve University

Jianye Zhang
Case Western Reserve University

Aditya Sharma
Washington University School of Medicine in St. Louis

Juan M. Angueyra
National Eye Institute

Alexander V. Kolesnikov
Washington University School of Medicine in St. Louis

See next page for additional authors

JGP Journal of General Physiology

RESEARCH ARTICLE

Retinoid isomerase inhibitors impair but do not block mammalian cone photoreceptor function

Philip D. Kiser[1,2], Jianye Zhang[2], Aditya Sharma[3], Juan M. Angueyra[4], Alexander V. Kolesnikov[3], Mohsen Badiee[5], Gregory P. Tochtrop[5], Junzo Kinoshita[6], Neal S. Peachey[1,6,7], Wei Li[4], Vladimir J. Kefalov[3], and Krzysztof Palczewski[2]

Visual function in vertebrates critically depends on the continuous regeneration of visual pigments in rod and cone photoreceptors. RPE65 is a well-established retinoid isomerase in the pigment epithelium that regenerates rhodopsin during the rod visual cycle; however, its contribution to the regeneration of cone pigments remains obscure. In this study, we use potent and selective RPE65 inhibitors in rod- and cone-dominant animal models to discern the role of this enzyme in cone-mediated vision. We confirm that retinylamine and emixustat-family compounds selectively inhibit RPE65 over DES1, the putative retinoid isomerase of the intraretinal visual cycle. In vivo and ex vivo electroretinography experiments in *Gnat1*$^{-/-}$ mice demonstrate that acute administration of RPE65 inhibitors after a bleach suppresses the late, slow phase of cone dark adaptation without affecting the initial rapid portion, which reflects intraretinal visual cycle function. Acute administration of these compounds does not affect the light sensitivity of cone photoreceptors in mice during extended exposure to background light, but does slow all phases of subsequent dark recovery. We also show that cone function is only partially suppressed in cone-dominant ground squirrels and wild-type mice by multiday administration of an RPE65 inhibitor despite profound blockade of RPE65 activity. Complementary experiments in these animal models using the DES1 inhibitor fenretinide show more modest effects on cone recovery. Collectively, these studies demonstrate a role for continuous RPE65 activity in mammalian cone pigment regeneration and provide further evidence for RPE65-independent regeneration mechanisms.

Introduction

Light perception by the vertebrate eye begins with a cis-to-trans photoisomerization of the retinylidene chromophore of photoreceptor cell visual pigments. This geometric change converts the opsin protein component of these pigments to an active signaling state, which is capable of initiating the phototransduction cascade with consequent changes in second messenger levels and plasma membrane potentials. In this way, a light stimulus is converted to an electrical signal, which is propagated to the brain for interpretation of the visual world. Photoreceptor signaling is sustained by a regeneration process that carries out the light-independent, endergonic conversion of trans-retinoid back to an 11-cis configuration, a pathway known as the retinoid or visual cycle (Saari, 2012; Kiser et al., 2014). The classic version of this pathway involves chemical transformations occurring in the retinal pigment epithelium (RPE) that are critical for the regeneration of rod visual pigments (Fig. 1; Kuhne, 1878). In this pathway, all-trans-retinaldehyde released from bleached visual pigments is converted to vitamin A, which is trapped in the RPE through the action of an esterifying enzyme called lecithin-retinol acyltransferase (LRAT; Saari and Bredberg, 1989). These retinyl esters serve as substrates for the membrane-bound enzyme RPE65 (RPE-specific 65-kD protein), which cleaves and isomerizes them to form 11-cis-retinol (Redmond et al., 1998). This cis-retinoid is further oxidized and then shuttled back to photoreceptor outer segments, where it combines with free opsins to form ground state pigments poised for subsequent light activation (Palczewski, 2006).

A conundrum exists regarding the role of RPE65 in cone visual pigment regeneration. On the one hand, the severely attenuated cone electroretinography (ERG) responses in *Rpe65* knockout mice (Redmond et al., 1998; Seeliger et al., 2001; Maeda et al., 2009) as well as humans (Jacobson et al., 2007, 2009) and

[1]Research Service, Louis Stokes Cleveland Veterans Affairs Medical Center, Cleveland, OH; [2]Department of Pharmacology, School of Medicine, Case Western Reserve University, Cleveland, OH; [3]Department of Ophthalmology and Visual Sciences, Washington University School of Medicine, Saint Louis, MO; [4]Retinal Neurophysiology Section, National Eye Institute, Bethesda, MD; [5]Department of Chemistry, College of Arts and Sciences, Case Western Reserve University, Cleveland, OH; [6]Cole Eye Institute, Cleveland Clinic, Cleveland, OH; [7]Department of Ophthalmology, Cleveland Clinic Lerner College of Medicine of Case Western Reserve University, Cleveland, OH.

Correspondence to Krzysztof Palczewski: kxp65@case.edu; Vladimir J. Kefalov: kefalov@wustl.edu; Philip D. Kiser: pdk7@case.edu.

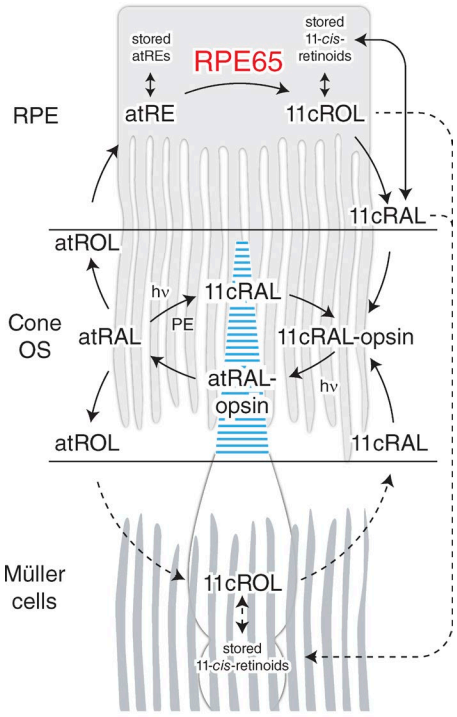

Figure 1. **Mechanisms for visual chromophore production in the retina relevant to cone pigment regeneration.** Cone-mediated vision is initiated by photoisomerization of 11-cis-retinaldehyde bound to cone visual pigments, a process that leads to pigment activation and initiation of phototransduction. Photoisomerization leads to the release of all-trans-retinaldehyde from the visual pigment, which must be regenerated to allow for sustained visual function. Two enzymatic systems are thought to contribute to 11-cis-retinaldehyde production for the regeneration of cone pigments. The classical RPE65-dependent visual cycle pathway involves enzymes and retinoid-binding proteins located in photoreceptor outer segments and the RPE. This pathway is also critically involved in rod pigment regeneration. The RPE can store 11-cis-retinoids either in the form of 11-cis-retinaldehyde or 11-cis-retinol complexed with cellular retinaldehyde-binding proteins or, in some species, as 11-cis-retinyl esters. A second cone-specific enzymatic pathway, which is believed to be RPE65 independent and mechanistically distinct from the classical visual cycle, may involve enzymes and binding protein components located in cones and Müller cells. This pathway could generate the 11-cis-retinoids that are present in Müller glia, but such compounds could also originate in the RPE and be transferred through the retina to the Müller cells. Müller cells can store 11-cis-retinoids by the same mechanisms as used by RPE, but the extent of 11-cis-retinyl ester formation is species dependent, typically being higher in diurnal animals. Selective regeneration of cone visual pigments relies on the unique ability of cones to use 11-cis-retinol delivered by Müller cells to form the necessary visual chromophore 11-cis-retinaldehyde. 11-cis-retinaldehyde also can be generated in situ in a light-dependent fashion via photoisomerization of all-trans-retinaldehyde-phosphatidylethanolamine Schiff base adducts. In this figure, solid lines indicate established pathways, whereas dashed lines indicate processes that are either hypothetical or not yet fully characterized. 11cRAL, 11-cis-retinaldehyde; 11cROL, 11-cis-retinol; atRAL, all-trans-retinaldehyde; atRE, all-trans-retinyl ester; atROL, all-trans-retinol; hν, a photon; PE, phosphatidylethanolamine.

dogs (Acland et al., 2005) with loss of function *RPE65* mutations, together with the apparent lack of cone pigment formation in *Nrl*$^{-/-}$*Rpe65*$^{-/-}$ mice (Wenzel et al., 2007; Feathers et al., 2008), suggest that RPE65 is an essential component of the cone pigment regeneration pathway, as is the enrichment of RPE65 expression and function in the cone-rich foveal region of the primate retina (Jacobson et al., 2007). Data showing enhanced isomerase activity for RPE65 from the cone-dominant chicken compared with orthologues from rod-dominant rodent species also suggest a mechanism whereby classical visual cycle activity can be tuned to match the high visual chromophore demands of cone photoreceptors (Moiseyev et al., 2008).

On the other hand, there are several lines of biochemical and electrophysiological evidence to suggest that the neurosensory retina possesses alternative visual cycle machinery devoted to cone pigment regeneration, indicating that there are RPE65-independent mechanisms for visual chromophore production (Fig. 1; Mata et al., 2002; Muniz et al., 2009; Wang et al., 2009). This alternative route of visual chromophore delivery is critically dependent on Müller glia (Jones et al., 1989; Das et al., 1992; Mata et al., 2002; Wang and Kefalov, 2009, 2011; Saari, 2012), and candidate enzymes of the mammalian pathway have recently been identified, including the putative isomerase sphingolipid delta(4)-desaturase 1 (DES1; Kaylor et al., 2013). Additional enzymes and potentially alternative enzymatic activities involved in cis-retinoid formation have also been identified in Müller cells of chicken (Muniz et al., 2009) and zebrafish (Takahashi et al., 2011) retina. More recent work has shown that 11-cis-retinaldehyde can also be generated nonenzymatically in situ within photoreceptor outer segments through the action of blue light on all-trans-retinaldehyde-phosphatidylethanolamine adducts (Kaylor et al., 2017). Notably, the emergence of ancestral cone pigments during chordate evolution (Lamb, 2013) is thought to have preceded the development of RPE65 and the classical visual cycle in vertebrates by several million years (Albalat, 2012; Poliakov et al., 2012b), indicating the existence of alternative chromophore regeneration pathway(s) that could be retained in extant species (Kusakabe et al., 2001). However, no direct genetic evidence yet demonstrates the involvement of alternative enzymes in cone pigment regeneration, and the existence of an RPE65-independent, cone-specific regeneration pathway remains controversial.

The rapid degeneration of cone photoreceptors that occurs in response to genetic perturbations of the RPE65 gene complicates the analysis of cone photoreceptor dependence on this enzyme (Cideciyan, 2010). Use of pharmacological agents to acutely block RPE65 function without direct effects on cone photoreceptor health offers an experimental strategy to overcome this limitation. Analysis of putative RPE65 isomerization intermediates has helped to identify retinylamine (Ret-NH_2) as a transition state analogue inhibitor of RPE65 (Golczak et al., 2005b). Subsequent studies led to the identification of a related but more potent inhibitor, emixustat (Bavik et al., 2015), which was developed as a visual cycle modulator for the treatment of dry, age-related macular degeneration (Kubota et al., 2012). The structure of this molecule in complex with RPE65 has provided a clear understanding of its mode of action as a competitive inhibitor of retinyl ester binding (Kiser et al., 2015). Likewise, the retinoic acid derivative fenretinide has been identified as a competitive inhibitor of DES1 activity (Rahmaniyan et al., 2011; Kaylor et al., 2013), although this molecule is known to interact with other molecular targets (Berni and Formelli, 1992; Dew et al., 1993; Poliakov et al., 2012a). Pharmacological approaches have previously been used to study isomerase activity in vitro (Gollapalli and Rando, 2003; Golczak

et al., 2005b, 2008; Muniz et al., 2009; Poliakov et al., 2011) as well as in mice (Golczak et al., 2005b; Mandal et al., 2011) and zebrafish (Schonthaler et al., 2007; Babino et al., 2015). However, the selectivity and potency of agents used in these studies were, in many cases, either unknown or not ideal. Emixustat and related derivatives such as MB-001 (Kiser et al., 2015), however, have well-validated modes of RPE65 inhibition with good in vivo activity and are therefore important new tools for studying the role of RPE65 in rod and cone visual pigment regeneration.

In this study, we determined the inhibitory specificity of Ret-NH_2/emixustat-family compounds toward RPE65 and then investigated how selective and acute suppression of the RPE-based visual cycle affects cone function and dark adaptation in mice and ground squirrels possessing rod- and cone-dominant retinas, respectively. We also investigated the effects of fenretinide treatment on cone function. These experiments allowed us to determine the relative importance of the RPE65-dependent visual cycle in acutely supplying visual chromophore to cones and supporting cone-mediated daytime vision without inducing photoreceptor degeneration.

Materials and methods

Chemicals and synthesis

Ret-NH_2 (Golczak et al., 2005b), QEA-B-001-NH_2 (Zhang et al., 2015b), emixustat, and MB-001 (Kiser et al., 2015) were synthesized according to previously described procedures. Fenretinide was purchased from Sigma-Aldrich or Toronto Research Chemicals, and the chemical identity was confirmed by optical spectroscopy. Standard laboratory chemicals were purchased from Sigma-Aldrich or USB and were of the highest available purity.

Retinoid isomerase activity assays

RPE65 retinoid isomerase activity was assayed as previously described (Stecher et al., 1999; McBee et al., 2000). Assays with ground squirrel RPE samples were performed using whole cell lysates as opposed to isolated microsomes because of the limited amount of material available.

RPE65 immunoblotting

Protein samples containing RPE65 were separated by SDS-PAGE on a 10% Tris-glycine polyacrylamide gel and then transferred to a 0.45-µm pore size polyvinylidene difluoride membrane. Phosphate-buffered saline containing 0.05% Tween 20 (Thermo Fisher Scientific) and 5% nonfat powdered milk was used as the blocking and incubation buffer. An in-house–generated RPE65 antibody (Golczak et al., 2010) at a 1:1,000 dilution was used for the primary incubation, which was subsequently detected with a horseradish peroxidase–conjugated anti–mouse IgG secondary antibody (Promega) and chemiluminescence reagent (Thermo Fisher Scientific).

Animal handling

Mice were housed in the animal facilities at the Case Western Reserve University School of Medicine, where they received a standard chow diet (LabDiet 5053) and were maintained under a 12-h light (~300 lux) and 12-h dark cycle; at the Washington University School of Medicine, where they received a standard chow diet (LabDiet 5053) and were maintained under a 12-h light (~20 lux) and 12-h dark cycle; or at the Cole Eye Institute animal facility, where they received LabDiet 2918 and were maintained under a 14-h light (~100 lux) and 10-h dark cycle. 13-lined ground squirrels (*Ictidomys tridecemlineatus*) were housed individually at the National Institutes of Health Veterinary Research and Resources Section, where they received a Cat Chow Complete (Nestlé Purina) diet and were kept in a 12-h light and 12-h dark cycle.

All animal procedures and experiments were approved by the Institutional Animal Care and Use Committees of Case Western Reserve University, the National Eye Institute, Washington University, or the Cleveland Clinic; conformed to the recommendations of the American Veterinary Medical Association Panel on Euthanasia; and were conducted in accordance with the Association for Research in Vision and Ophthalmology Statement for the Use of Animals in Ophthalmic and Visual Research.

Liver microsome isolation

Liver microsomes from *Lrat*$^{-/-}$ mice on a C57BL/6J genetic background were used as the enzyme source for the DES1 activity assays to eliminate potential LRAT-dependent acylation of test compounds (Batten et al., 2004; Golczak et al., 2005a; Zhang et al., 2015b). Four 8-wk-old mice were euthanized by CO_2 asphyxiation and cervical dislocation, and their livers (4.6 g in total) were removed by dissection, washed in ice-cold phosphate-buffered saline, flash frozen in liquid nitrogen, and stored at −80°C. Liver microsomes were isolated by differential centrifugation as previously described (Schulze et al., 2000). The microsomes then were suspended in 100 mM sodium phosphate, pH 7.4, to a final protein concentration of 15 mg/ml as determined by the Bradford assay with BSA used as the standard. Microsome preparations were flash frozen in liquid nitrogen and stored at −80°C.

DES1 activity assays

Based on the finding that the retinol isomerase activity of DES1 is competitive with its dihydroceramide desaturase activity (Kaylor et al., 2013), the influence of RPE65 inhibitors on DES1 catalytic function was assessed by measuring DES1 dihydroceramide activity in the presence of these compounds with a radioactivity-based assay in which ^3H is released from 4,5-^3H-dihydroceramide in the form of tritiated water as a result of DES1 catalytic activity. This assay used mouse liver microsomes isolated as described in the preceding section along with a substrate, *N*-octanoyl-dihydroceramide (C_8-dihydroceramide), which has been previously shown to compete with retinol for binding to the DES1 active site (Fig. S1 A; Schulze et al., 2000; Kaylor et al., 2013). The dihydroceramide desaturase activity from this source was linear over the assay time course and approximately proportional to the enzyme concentration (Fig. S1 B) and also exhibited steady-state kinetic parameters similar to those previously reported for rat liver microsomes (Fig. S1 C; Rahmaniyan et al., 2011). Reactions were performed in 20 mM sodium phosphate, pH 8, containing 50 mM NaCl, 50 mM sucrose, 2 mM reduced nicotinamide adenine dinucleotide (NADH), and 120 µg microsomal protein in a total volume of 500 µl. C_8-dihydroceramide (Matreya),

solubilized in 100 mM sodium phosphate, pH 7.4, containing 179 mM 3-[(3-cholamidopropyl)dimethylammonio]-1-propanesulfonate (CHAPS; Anatrace), was used as a substrate for the reaction. 1 µl ethanolic solution of 4,5-^{3}H-C_8-dihydroceramide (1 µCi/µl; American Radiolabeled Chemicals) was added to 22.2 µl of solubilization buffer, and the mixture was vortexed for 30 s. 1 µl of the diluted radiolabeled substrate (0.043 µCi, ∼150,000 dpm) was used per reaction. The final concentration of CHAPS in the reaction mixtures was fixed at 1.59 mM. For inhibitor studies, the test compounds were delivered into the reaction system in DMSO, and the sample was mixed by brief vortexing. The final DMSO concentration in the assay system was fixed at 0.2% vol/vol, a level that did not affect DES1 activity. Reaction mixtures were preincubated for 10 min at 37°C, and reactions were then initiated by addition of substrate followed by brief vortexing. Reactions were performed at 37°C with 550 rpm shaking for 20 min in 1.5-ml tubes. Reactions performed in the absence of NADH or with heat-treated microsomes were used to determine the background level of the assay. Reactions were terminated with 100 µl of 72% trichloroacetic acid followed by vortexing. The resulting precipitates were sedimented by centrifugation at 16,100 *g* for 4 min. Supernatants were removed and added to 1 ml of 0.4 M Na_2HPO_4 to partially deacidify the solution. The resulting mixtures were then applied to a 500-mg, 3-ml Bond Elut C18 column (Agilent) preconditioned with 2 ml of 100% MeOH followed by equilibration with 2 ml Millipore water. Liquid was drawn through the column with a vacuum manifold operating at ≤5 inches of Hg. 2 ml Millipore water was then drawn through the column to capture residual aqueous radioactivity. The entire flow-through volume was added to 10 ml of Ultima Gold XR scintillation cocktail (Perkin-Elmer) and mixed by shaking. Scintillation recordings were made with a Beckman LS6500 instrument.

In vivo ERG of *Gnat1*$^{-/-}$ mice

3-mo-old *Gnat1*$^{-/-}$ mice on a BALB/c background (Leu450 variant of RPE65) were dark adapted overnight and then anesthetized with an intraperitoneal (IP) injection of a ketamine (100 mg/kg) and xylazine (20 mg/kg) mixture. Pupils were dilated with a drop of 1% atropine sulfate. The mouse body temperature was maintained at 37°C with a heating pad. ERG responses were recorded from both eyes by contact electrodes connected to the cornea by a drop of Gonak solution. Full-field ERGs were performed with a UTAS BigShot apparatus (LKC Technologies) using Ganzfeld-derived test flashes of calibrated green 530-nm light-emitting diode (LED) light ranging from 0.24 to 7.45 cd·s/m^2. Cone b-wave flash sensitivity (S_f) was first calculated in the dark as follows:

$$S_f = R/(R_{max} \cdot I),$$

where R is the cone b-wave dim flash response amplitude, R_{max} is the maximal response amplitude for that retina obtained with the brightest white light stimulus of the Xenon Flash tube (700 cd·s/m^2), and I is the flash strength. Then, >90% of the M-cone pigment was bleached by a 30-s exposure to 520-nm LED light focused at the surface of the cornea. The bleaching fraction was estimated with the following equation:

$$F = 1 - e^{-I \cdot P \cdot t},$$

where F is the fraction of bleached pigment, t is the duration of the exposure to light (in seconds), I is the bleaching light intensity of unattenuated 520-nm LED light (∼1.3 × 10^8 photons µm^{-2}s^{-1}), and P is the photosensitivity of the mouse cone at the wavelength of peak absorbance (7.5 × 10^{-9} µm^2), adopted from Nikonov et al. (2006). After the bleach, recovery of cone b-wave S_f was followed in the dark for up to 1 h. Mice were reanesthetized once (at 20 min after bleach) with a smaller dose of ketamine (approximately half the initial dose), and a 1:1 mixture of phosphate-buffered saline and Gonak solutions was gently applied to the eyes to protect them from drying and to maintain electrode contacts.

To test cone function under extended photopic conditions, white-background Ganzfeld illumination (300 cd/m^2) was applied to dark-adapted mice continuously for 30 min, and the cone b-wave S_f change was monitored during this period. After the exposure, recovery of cone b-wave S_f was monitored in the dark for up to 1 h, and anesthesia was reapplied every 30 min.

Ret-NH_2 was dissolved before each experiment in DMSO to 5 µg/µl, and 50 µl of this solution was administered by IP injection in the dark, followed by a period of 22–26 h of dark adaptation before recordings. The other compounds were delivered similarly in 50 µl DMSO. Their final concentrations were 4 µg/µl emixustat, 4 µg/µl MB-001, or 40 µg/µl QEA-B-001-NH_2. Control animals were injected with 50 µl DMSO and processed in the same way as drug-treated mice.

Ex vivo ERG recordings from isolated *Gnat1*$^{-/-}$ mouse retinas

3-mo-old *Gnat1*$^{-/-}$ mice were dark adapted overnight and sacrificed. A whole retina was removed from each mouse eyecup under infrared illumination and stored in oxygenated aqueous L15 solution (13.6 mg/ml, pH 7.4; Sigma-Aldrich) containing 0.1% BSA at room temperature. The retina was mounted on filter paper with the photoreceptor side up and placed in a perfusion chamber between two electrodes connected to a differential amplifier. The preparation was perfused with Locke's solution containing 112.5 mM NaCl, 3.6 mM KCl, 2.4 mM $MgCl_2$, 1.2 mM $CaCl_2$, 10 mM HEPES, pH 7.4, 20 mM $NaHCO_3$, 3 mM sodium succinate, 0.5 mM sodium glutamate, 0.02 mM EDTA, and 10 mM glucose. This solution was supplemented with 2 mM L-glutamate and 10 µM DL-2-amino-4-phosphonobutyric acid to block postsynaptic components of the photoresponse (Sillman et al., 1969) and with 20 µM $BaCl_2$ to suppress the slow glial PIII component (Nymark et al., 2005). The perfusion solution was continuously bubbled with a 95% O_2/5% CO_2 mixture and heated to 36–37°C.

Light stimulation was applied in 20-ms test flashes of calibrated 505-nm LED light. The light intensity was controlled by a computer in 0.5 log unit steps. To monitor the recovery of cone a-wave flash sensitivity (S_f, defined as for the b-wave above) after the bleach, >90% of M-cone visual pigment was bleached with a 3-s exposure to 505-nm light. Photoresponses were amplified by a differential amplifier (DP-311; Warner Instruments), low-pass filtered at 30 Hz (eight-pole Bessel), digitized at 1 kHz, and stored on a computer. Data were analyzed with Clampfit 10.4 (Molecular Devices) and Origin 8.5 (OriginLab) software.

Ret-NH_2 and DMSO were administered to each dark-adapted mouse by IP injection as described above, followed by a further period of 15–17 h of dark adaptation before physiological recordings. Fenretinide was dissolved in DMSO and acutely added to the isolated, dark-adapted retina, which was flat mounted on filter paper with the photoreceptor side up and placed into 2 ml L15 solution containing 1% BSA (final concentrations of the drug were 100 µM or 650 µM, and that of DMSO was 1.3%). After preincubation for 1 h at room temperature, the retina was exposed to moderate 520-nm light for 2 min to bleach the bulk of cone pigment, and trans-retinal ERG recordings were performed after another hour in darkness. Control experiments were performed in an identical way but with DMSO only. Some retinas were treated with fenretinide or DMSO for 1 h but not bleached before recordings.

In vivo ERGs in wild-type mice

C57BL/6J mice aged 2 or 7 mo were anesthetized with ketamine (80 mg/kg) and xylazine (16 mg/kg). Mydriatic eye drops (1% tropicamide–2.5% phenylephrine–1% cyclopentolate or 1% tropicamide alone) were used to dilate the pupil. ERGs were obtained using a stainless steel active electrode that contacted the corneal surface through a layer of 1% carboxymethylcellulose or normal saline. Needle electrodes placed in the cheek and tail provided reference and ground leads, respectively. Strobe stimuli were presented in a Ganzfeld (LKC Technologies), either in darkness or under photopic conditions where stimulus flashes were superimposed on a steady adapting field (20 cd/m^2) after at least 5 min of light adaptation. Responses were amplified, averaged, and stored using an LKC Technologies UTAS E-3000 signal averaging system. Under dark-adapted conditions, stimulus strength ranged from −3.6 to 2.1 log cd·s/m^2. Across this range, the interstimulus interval increased from 4 to 65 s with increasing flash luminance, whereas the number of averaged consecutive responses decreased over the same stimulus range from 20 at the lowest flash luminance to a single response at the highest strength stimulus. Under light-adapted conditions, stimulus strength ranged from −0.4 to 1.9 log cd·s/m^2, and flashes were presented at 2 Hz. For each light-adapted stimulus condition, up to 50 consecutive responses were averaged.

Baseline light-adapted ERGs were recorded from each mouse. Mice were injected IP in the morning with 50 µl of vehicle (10% DMSO in normal saline) or MB-001 (160 µg/mouse/day) for three successive days and kept under normal cyclic lighting conditions (14 h light/10 h dark). Both male and female mice were used. The morning after the final injection, mydriatic eye drops were used to dilate the pupils. Mice were placed in darkness after one of two light exposures. Bleach mice were exposed to a 10-min × 10,000-lux bleach, whereas no bleach mice were not. After a 6-h dark adaptation, mice were anesthetized as described above, and a series of dark- and light-adapted ERGs were recorded.

For fenretinide experiments, mice were given either 6 mg fenretinide (~267 mg/kg) or vehicle (50% DMSO and 25% ethanol in water) by IP injection for three consecutive days. On the third day, 1 h after the final dose, the animals were given mydriatic eye drops and then were subjected to a 10-min × 10,000-lux photobleach. The animals were then allowed to dark adapt for 6 h before ERG recordings.

To test the impact of MB-001 treatment on fully dark-adapted rod responses without a prior photobleach or other light exposure during the period of drug exposure, MB-001 at a dose of 8 mg/kg was given to 2-mo-old C57BL/6J mice for two consecutive days via IP injection. These mice were housed in darkness for 24 h before drug administration, and the drug was administered under dim red light. After the recording of dark-adapted ERGs 2 h after the second dose using the protocol described above, the animals were subjected to a 10-min × 10,000-lux photobleach under anesthesia and then allowed to dark adapt for 22 h. After this period, scotopic ERGs were remeasured. For MB-001–treated mice, dark-adapted ERGs were also measured again after a 2-wk drug washout period.

In vivo ERGs in squirrels

Healthy 13-lined ground squirrels (*I. tridicemlineatus*, 3–6 mo old, during the summer season) of both sexes were used for ERG recordings. Before ERG recording, the animals were anesthetized using 3–4% isofluorane suspended in pure oxygen, and their pupils were dilated using ophthalmic 1% tropicamide and 2.5% phenylephrine, with 0.5% proparacaine used as a local anesthetic. Body temperature was maintained at 37°C with a warm bed, and the heart rate was monitored continuously. ERG signals were measured differentially using gold electrodes coated with hydroxypropyl-methylcellulose that were pressed into the cornea of both eyes, and a subdermal scalp tungsten needle was the reference electrode. The Espion Color-Dome system (Diagnosys LLC) was used for data acquisition and stimulation. The data were sampled at a rate of 1,000 Hz and low-pass filtered at 200 Hz. The built-in xenon lamp was used for stimulation with flashes of <2 ms in duration and spanning 0.1–4,000 cd·s/m^2 in intensity. In preliminary experiments with normal squirrels, exposure to a bright and broadband LED source (Migthex White LED 5 500K at maximal intensity, focused on one eye at a distance of 10 cm and for a 10-min period) successfully suppressed the response (>90%) to a midintensity flash (100 cd·s/m^2), with near-complete recovery of responses in the following 10 min. This treatment was adopted as our bleaching protocol. The recovery of ERG sensitivity was monitored after the photobleach by delivering midsaturating flashes (100 cd·s/m^2 except for one high-dose MB-001–treated animal in which 300 cd·s/m^2 was used) every 1.5 s, with periodic gaps required to save data and restart the stimulation protocol.

After recording baseline ERGs, the animals were injected with MB-001 or vehicle using two different treatment protocols. In the first, MB-001 at a dose of 8 mg/kg/day or the vehicle solution (10% vol/vol DMSO in 0.9% saline) was injected IP for three consecutive days in four squirrels. During this time, the animals were kept under normal cyclical lighting conditions. After the 3 d of treatment, ERGs were recorded again. After a 6-wk washout period, the treatments were crossed over in the same four subjects to perform a paired analysis, repeating the same procedures but opposite treatments. After the last recording, the squirrels were sacrificed by decapitation after deep anesthesia with isofluorane, and their eyes were collected and immediately immersed into liquid nitrogen. The eyes were stored at −80°C

until quantification of MB-001 levels. In the second treatment protocol, either MB-001 at doses of 8 mg/kg/day or 80 mg/kg/day or vehicle (50% vol/vol DMSO and 25% vol/vol EtOH in water) was injected IP for three consecutive days. A fenretinide treatment group (166 mg/kg/day delivered IP in the same vehicle) was also included in the second protocol. During this time, the animals were kept under normal cyclical lighting conditions. ERGs were recorded on the third day of treatment, 2 h after the final injection. After the last recording, the squirrels were sacrificed by decapitation after deep anesthesia with isofluorane. Their eyes were enucleated, and after removal of the cornea, lens, and vitreous and partial removal of the retina, the RPE was collected for RPE65 activity assays.

ERG data were analyzed in MATLAB (MathWorks) with custom scripts and colormaps designed and made publicly available by Matteo Niccoli (Niccoli, 2018). Three to five trials per flash intensity were averaged after baseline subtraction. The averaged traces were used to identify the amplitude of the a-wave as the maximal downward deflection in the first 30 ms after stimulation and the amplitude of the b-wave as the maximal upward deflection up to 100 ms after stimulation. To assess the effect of pharmacological treatment, the difference before and 10 min after the bleaching protocol (expressed as a percentage) was calculated for both the a- and b-wave amplitudes at every light intensity used for stimulation. This difference was calculated only for flash intensities >10 cd·s/m^2. Below this intensity, ERG responses were small and noisy. Recovery data spanning the full 600-s time window were fit with the exponential rise to plateau equation

$$F(t) = a + c \times \left[1 - \exp(-t/\tau)\right]$$

using the lsqcurvefit routines in MATLAB, with a (baseline shift variable), c (fractional recovery at t = +∞), and τ (the recovery time constant) variables treated as free parameters. Although cone sensitivity recovery obeys a rate-limited kinetic model (Mahroo and Lamb, 2004), reasonable fits were obtained here with the simpler exponential function. The recovery fraction was calculated as the b-wave amplitude 500–600 s after bleach divided by the prebleach b-wave amplitude.

Quantification of MB-001 in squirrel and mouse eyes

Eyes from ground squirrels or C57BL6/J mice that had received three consecutive days of IP MB-001 treatment (8 mg/kg/day) were homogenized in 3 ml of 10 mM sodium phosphate buffer, pH 7.4, containing 50% vol/vol methanol and hydroxylamine (50 mM). After adding 4 ml brine, the resulting mixture was extracted twice with 4 ml ethyl acetate. The combined extracts were dried in vacuo and reconstituted in 400 µl ethanol containing 2 nmol emixustat as the internal standard. This solution (100 µl) was analyzed by liquid chromatography–electrospray ionization tandem mass spectrometry with a Finnigan LXQ mass spectrometer (Thermo Fisher Scientific) and a 4.6 × 150–mm ZORBAX Eclipse XDB-C18 column (Agilent) with a gradient of acetonitrile in water (0–100% in 20 min) as the eluent at a flow rate of 0.5 ml/min. Amounts of MB-001 were quantified based on a standard curve representing the relationship between the amount of MB-001 and the ratio of the corresponding selected reaction monitoring peak areas of MB-001 (m/z 304.2→257.2) to emixustat (m/z 264.2→246.2).

Online supplemental material

Fig. S1 shows validation of the DES1 activity assay. Fig. S2 shows the effects of RPE65 inhibitors on DES1 enzymatic function. Fig. S3 shows the effects of MB-001 on dark-adapted mouse ERG responses. Fig. S4 shows the impact of MB-001 treatment on ERG responses in ground squirrels after the multiday dosing schedule used in wild-type mice. Fig. S5 shows the standard curve for MB-001 quantification. Fig. S6 shows the quantification of MB-001 levels in mouse and squirrel eyes. Table S1 summarizes the kinetic data presented in Fig. S2.

Results

Emixustat derivatives selectively inhibit RPE65 over DES1

Although the inhibitory activity of emixustat toward RPE65 has been studied extensively, its selectivity for this enzyme has not been established. Specifically, it is unknown whether emixustat or its derivatives also inhibit DES1. We therefore determined the influence of these RPE65 inhibitors on DES1 catalytic function (Fig. 2 A). We observed that MB-001 and emixustat had little or no inhibitory activity toward DES1, even at a concentration of 100 µM (Fig. 2 B), whereas RPE65 activity was drastically reduced by these compounds at a concentration of 10 µM (Fig. 2 C); the latter finding is consistent with prior data (Kiser et al., 2015; Zhang et al., 2015b). Conversely, the known DES1 inhibitor fenretinide (Rahmaniyan et al., 2011) strongly suppressed DES1 dihydroceramide desaturase activity at a concentration of 10 µM (Fig. 2 B) but had minimal effects on RPE65 retinoid isomerase activity (Fig. 2 C), confirming previous results (Golczak et al., 2008). Inhibition by Ret-NH$_2$ was intermediate between these two extremes, with ∼50% inhibition of DES1 activity achieved at a concentration of 100 µM and slightly less RPE65 inhibition at a concentration of 10 µM compared with the emixustat derivatives. The K_i values and modes of inhibition of the RPE65 inhibitors toward DES1 activity are summarized in Fig. S2 and Table S1. These data establish the utility of emixustat derivatives in selectively blocking RPE65-driven retinoid isomerization.

Impact of retinoid isomerase inhibition on cone dark adaptation after a brief step bleach

Having established the selectivity of Ret-NH$_2$, emixustat, and MB-001 toward RPE65, we next used ERG to investigate how their inhibition of the classical RPE visual cycle affects cone photoreceptor function. To facilitate isolation of the cone component of the ERG response, these experiments were performed with mice lacking the α subunit of rod transducin (*Gnat1*$^{-/-}$), an essential component of the rod phototransduction cascade. Deletion of the transducin α subunit blocks rod responses while preserving the structure of the retina as well as cone signaling (Calvert et al., 2000).

First, we recorded cone b-wave responses from dark-adapted *Gnat1*$^{-/-}$ mice by in vivo ERGs and estimated their photopic b-wave flash sensitivity. Treatment of mice with Ret-NH$_2$ had no detrimental effect on the function of cones under dark-adapted

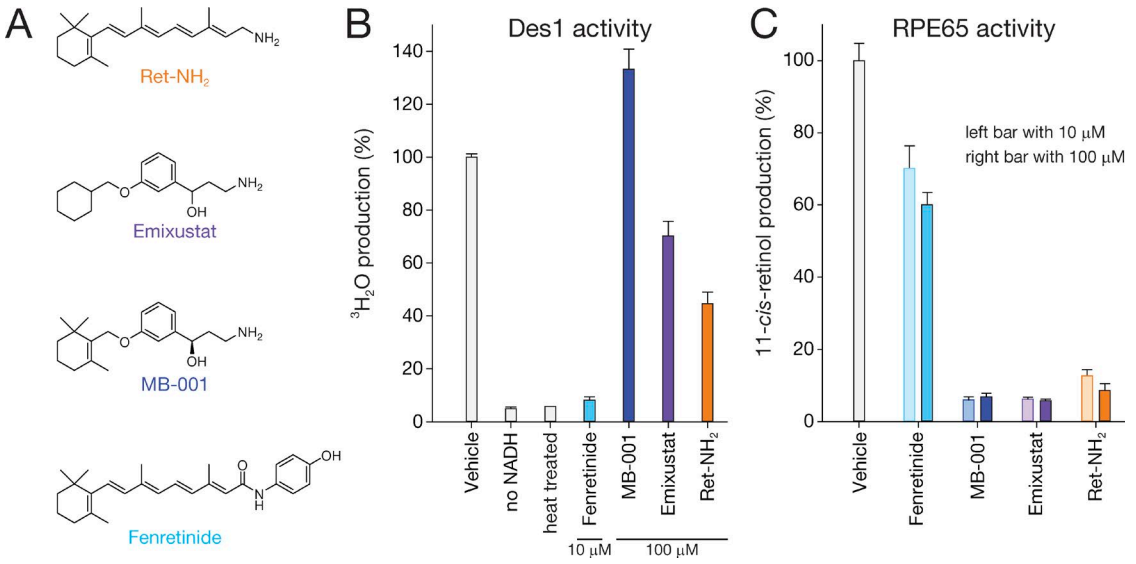

Figure 2. **Selectivity of RPE65 and DES1 inhibitors. (A)** Chemical structures of RPE65 and DES1 inhibitors used in this study. **(B)** Inhibitory effects of retinoids, emixustat, and emixustat derivatives on DES1 activity in liver microsomes from 8-wk-old *Lrat*$^{-/-}$ mice. Fenretinide, a known DES1 inhibitor, at a concentration of 10 μM suppressed DES1 activity nearly as well as heat treatment or omission of the required NADH cofactor. RPE65 inhibitors, in contrast, had less pronounced effects on activity. Assays shown here were performed at a fixed substrate concentration of 0.5 μM. Activity levels are normalized to that of the DMSO-only control samples. DMSO, at the concentration used in these assays (0.2% vol/vol), did not affect DES1 activity. **(C)** Inhibitory effects of retinoids, emixustat, and emixustat derivatives on 11-cis-retinol production in RPE microsomes. Compounds at final concentrations of 10 μM or 100 μM were incubated with RPE microsomes and 20 μM all-trans-retinol. Activities are normalized to DMSO-only treated samples. The bar graphs show mean values, and error bars represent SDs from at least three separate experiments.

conditions, as their sensitivity was not suppressed compared with that of DMSO-treated controls (Fig. 3 A). Mice then were exposed to brief bright light to bleach >90% of their visual pigment. This resulted in a substantial initial desensitization, followed by progressive recovery as the cone visual pigments were gradually regenerated. Comparison of the time course of cone-driven b-wave sensitivity recovery revealed that treatment with Ret-NH_2 suppressed the late phase of cone dark adaptation relative to vehicle-treated controls. As a result, the final level of cone sensitivity 1 h after the bleach was twofold lower in Ret-NH_2–treated mice than in control mice treated with DMSO (Fig. 3 A). This result is consistent with the view that, in mice, the late phase of cone dark adaptation after a brief step bleach is mediated by the classical RPE visual cycle. In contrast, the early phase of cone dark adaptation over the first ∼10 min after the bleach was not suppressed by treatment with Ret-NH_2. Using data from salamander cones (Kefalov et al., 2005), the recovery of cone sensitivity at this time point suggests that >50% of the cone visual pigment was regenerated despite inhibition of the RPE visual cycle. This finding suggests that after a step bleach, the early component of mouse cone dark adaptation is independent of RPE65 (i.e., not acutely dependent on continuous RPE65 activity).

The initial component of cone dark adaptation in vivo is thought to be driven by the intraretinal visual cycle (Kolesnikov et al., 2011). To confirm that this part of cone recovery is independent of the RPE, we examined the dark adaptation of cones in isolated retina after a step bleach. Under these conditions, the RPE is removed and the RPE visual cycle does not contribute to recovery, leaving the intraretinal visual cycle as the sole source of chromophore driving cone pigment regeneration. Comparison of retinas from vehicle- and Ret-NH_2–treated mice revealed identical time courses of cone dark adaptation (Fig. 3 B). Thus, Ret-NH_2 did not affect cone dark adaptation in the isolated retina, consistent with our finding that Ret-NH_2 does not effectively inhibit DES1. Rather, these findings indicate that the early rapid phase of cone dark adaptation after a step bleach is independent of RPE65 and is instead driven by the intraretinal visual cycle. Using the same ex vivo system, we also investigated the impact of DES1 inhibition by fenretinide on cone dark adaptation. Compared with vehicle-treated retinas, those exposed to 100 μM fenretinide exhibited a modest decrease in photosensitivity (Fig. 4). Photosensitivity was further decreased only slightly at a concentration of 650 μM, indicating that the effect had plateaued. These results further support a physiological role for DES1 in cone recovery mediated by the intraretinal visual cycle.

Emixustat and MB-001 exhibited even greater inhibitory potency and selectivity toward RPE65 compared with Ret-NH_2 (Fig. 2). Like Ret-NH_2, both emixustat (Fig. 5 A) and MB-001 (Fig. 5 B) inhibited the late phase of cone dark adaptation, but neither compound slowed early recovery after the photobleach. Ret-NH_2, emixustat, and MB-001 contain primary amine functional groups that are capable of directly reacting with retinaldehyde to form Schiff base adducts. To rule out the possibility of retinaldehyde sequestration giving rise to the late-phase dark adaptation effects, we tested QEA-B-001-NH_2, a compound that functions as a retinaldehyde sequestrant without inhibiting RPE65 (Zhang et al., 2015a). No suppression of cone dark adaptation in mice treated with QEA-B-001-NH_2 was observed (Fig. 5 C). These observations demonstrate that the early component of mouse cone dark adaptation in the intact eye after a

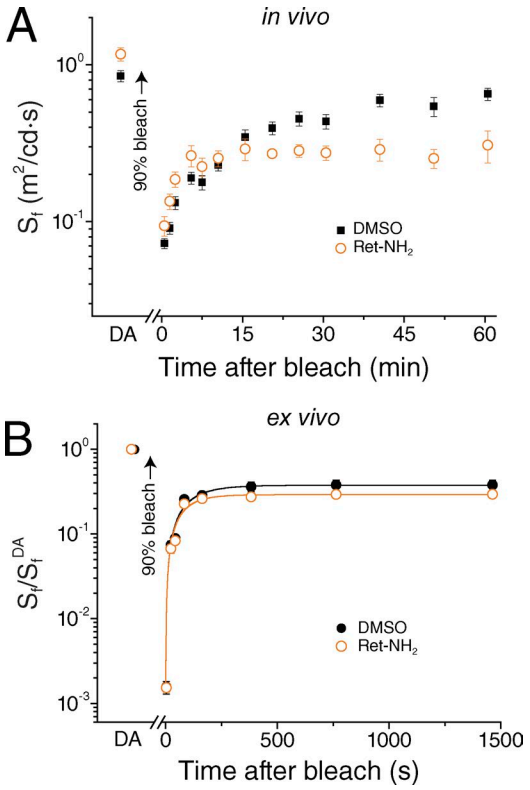

Figure 3. **Effect of Ret-NH_2 on mouse cone dark adaptation. (A and B)** Cone b-wave ERG responses were recorded in vivo (A), and cone a-wave ERG responses were recorded ex vivo (B). Sensitivity in each case was estimated as the ratio of the dim flash response and the corresponding flash intensity and further normalized to the maximal ERG response amplitude. Rod transducin α-deficient mice (*Gnat1*$^{-/-}$) were used to isolate the cone-specific component of the light responses. Mice (3 mo old) were dark adapted overnight, injected with 50 µl DMSO or Ret-NH_2 dissolved in DMSO to 5 µg/µl, and then kept in darkness for 22–26 h. After determining the sensitivity in the dark-adapted state, we exposed the eyes or isolated retinas for 30 s to bright 520-nm light estimated to bleach >90% of their visual pigment. Episodic dim flash stimulation was then used to follow the recovery of cone b-wave sensitivity in vivo (A) in mice treated with DMSO (n = 16) or with Ret-NH_2 (n = 10). Ret-NH_2 did not affect the early phase of cone dark adaptation driven by the intraretinal visual cycle but blocked its late phase, driven by the RPE visual cycle. Recovery of cone a-wave sensitivity ex vivo (B) was measured in isolated retinas from mice treated with DMSO (n = 7) or with Ret-NH_2 (n = 6). Ret-NH_2 did not affect the dark adaptation of cones in isolated retina. Data are presented as means ± SEM.

brief step bleach is driven by an RPE65-independent mechanism, whereas RPE65 contributes substantially to the late-phase recovery process.

Impact of RPE65 inhibition on cone function during extended photopic conditions

In their normal daily function, cones are rarely exposed to such brief, intense light exposures as the ones used in the preceding experiments. Thus, to test the efficiency of chromophore supply to cones under more physiological conditions, we exposed mice to 30 min of bright background light followed by a period of dark adaptation. Inefficient pigment regeneration in this case should result in gradual depletion of cone visual pigment and progressive cone desensitization during light exposure (Kolesnikov et al., 2015), as well as a delay in the subsequent cone dark adaptation upon extinction of the background light. In DMSO-treated *Gnat1*$^{-/-}$ mice, this protocol resulted in an ∼100-fold cone desensitization caused by light adaptation in bright background (Fig. 6 A, black circles). However, cone sensitivity remained stable for the duration of the background light, indicating sustained pigment regeneration. Upon the return to darkness, cone sensitivity recovered gradually over the next 30 min as cone pigment regenerated. Notably, treatment with emixustat did not compromise the ability of cones to maintain their sensitivity during the 30-min exposure to bright light (Fig. 6 A). Thus, cones were able to sustain robust function in bright light despite blockade of the RPE visual cycle by emixustat. All phases of cone dark adaptation upon return to darkness were delayed in emixustat-treated mice compared with vehicle-treated controls, suggesting an important role of the RPE visual cycle for cone pigment regeneration in these conditions. Similar experiments with MB-001 yielded comparable results; however, we observed a subtle and gradual desensitization of the cones during the 30 min of photopic exposure (Fig. 6 B). Finally, we also tested how cone function under photopic conditions is affected by the all-trans-retinaldehyde sequestrant QEA-B-001-NH_2. Consistent with the inability of this compound to inhibit cone dark adaptation after a step bleach (Fig. 5 C), QEA-B-001-NH_2 also had no effect on cone function during prolonged light exposure (Fig. 6 C). The subsequent dark adaptation of cones also was comparable in QEA-B-001-NH_2– and DMSO-treated mice.

Effects of retinoid isomerase inhibitor treatment on wild-type mouse photoreceptor responses

As a prelude to the evaluation of multiday RPE65 inhibitor treatment on cone function in the cone-dominant ground squirrel, we tested RPE65 inhibitor treatment on ERG responses in wild-type C57BL/6J mice. For these studies, we used MB-001 because of its strongly selective inhibitory activity toward RPE65 (Fig. 2 and Table S1).

We recorded a series of dark-adapted (Fig. 7) and light-adapted (Fig. 8) ERGs from mice treated with vehicle and then exposed to a bleach, or from mice treated with MB-001 with or without a bleach exposure. In vehicle-treated mice, the dark-adapted ERG was composed of two major components: a negative polarity a-wave followed by a positive polarity b-wave (Fig. 7 A).

The a-wave reflects the light-induced closure of ion channels along the rod outer segments, and the b-wave reflects the mass response of depolarizing bipolar cells (Abd-El-Barr et al., 2009). Rod recovery after a strong photobleach is an established surrogate for the ability of RPE65 to synthesize 11-cis-retinol, as the rate of rhodopsin regeneration after a full bleach is dependent on the expression level and activity of RPE65 (Wenzel et al., 2001; Lyubarsky et al., 2005). Compared with ERG responses obtained from vehicle-treated mice, which were comparable to prebleach responses, the ERG a- and b-wave amplitudes were markedly reduced in mice given MB-001 and subjected to a photobleach (Fig. 7, A–C). Although clear signals were seen in these animals, the responses were reduced in amplitude, and their waveforms closely resembled those obtained in *Gnat1*$^{-/-}$ mice, which lack rod-mediated function (Calvert et al., 2000; Wu et al., 2004). The

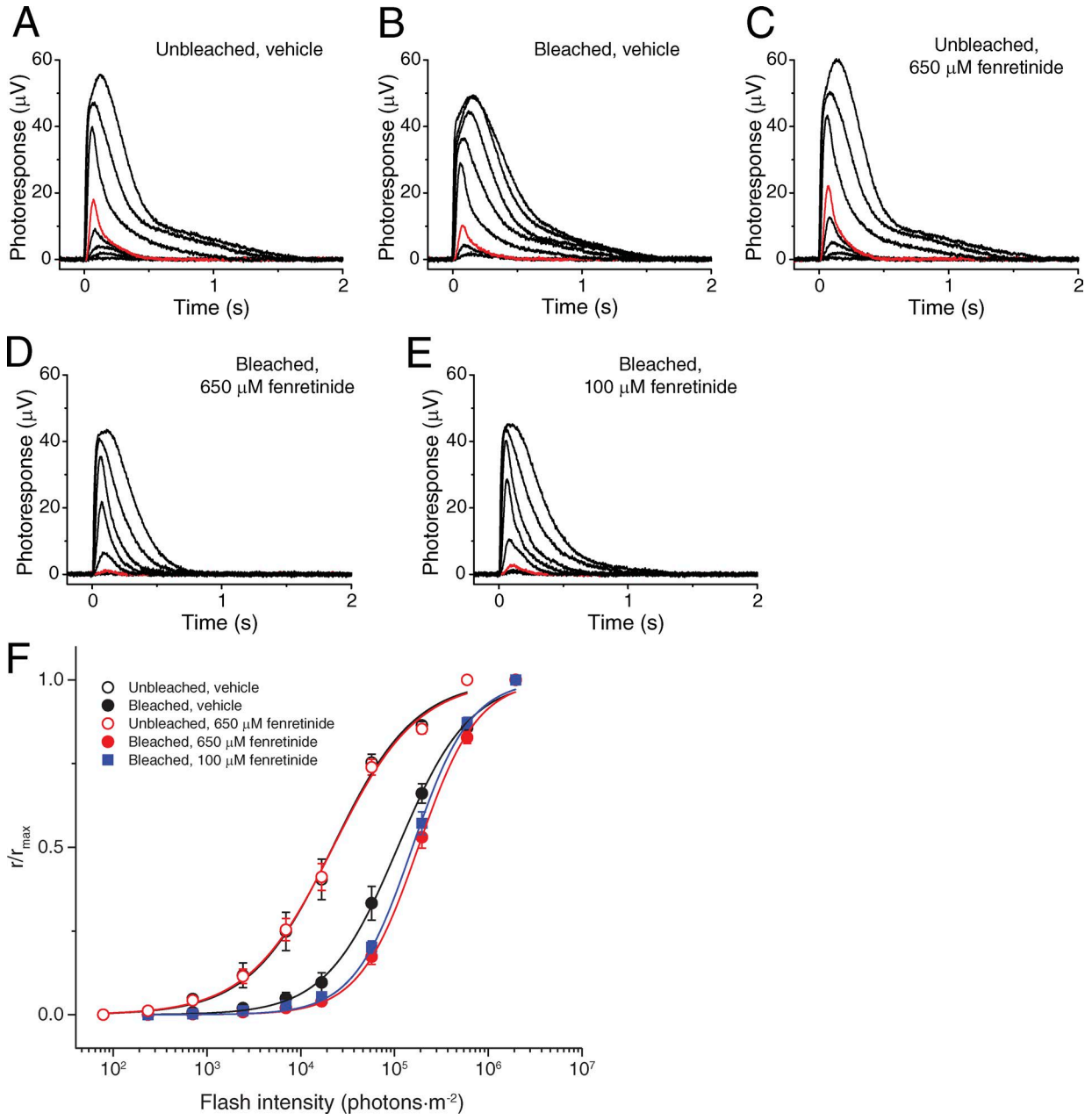

Figure 4. **Effect of fenretinide on cone dark adaptation in isolated retina. (A–E)** Representative families of ex vivo cone ERG responses from *Gnat1*$^{-/-}$ mouse retinas under specified conditions. **(A and C)** Test flashes of 505-nm light with intensities of 235, 705, 2.4 × 10^3, 7.0 × 10^3, 1.7 × 10^4, 5.7 × 10^4, 2.0 × 10^5, and 6.0 × 10^5 photons/μm^2 were delivered at time 0. **(B, D, and E)** Test flashes of 505-nm light with intensities of 2.4 × 10^3, 7.0 × 10^3, 1.7 × 10^4, 5.7 × 10^4, 2.0 × 10^5, 6.0 × 10^5, 2.0 × 10^6, and 5.7 × 10^6 photons/μm^2 were delivered at time 0. In all panels, responses to 1.7 × 10^4 photons/μm^2 light are shown in red for comparison of cone sensitivity recovery after a bleach. **(F)** Averaged cone intensity–response functions (mean ± SEM) for dark-adapted conditions treated for 1 h with 1.3% DMSO (vehicle control, open circles; *n* = 6) or with 650 μM fenretinide (open red circles; *n* = 6) and 1 h after a bleach of retinas preincubated for 1 h in 1.3% DMSO (vehicle control, closed black circles; *n* = 11), 100 μM fenretinide (closed blue squares; *n* = 6), or 650 μM fenretinide (closed red circles; *n* = 9). The recovery of cone sensitivity was suppressed by treatment with fenretinide at both 100 μM and 650 μM.

overall amplitudes of the dark-adapted ERG responses of mice administered MB-001 but not exposed to the bleach were intermediate between vehicle- and MB-001–treated mice that underwent the bleach, with rod contributions to the waveforms clearly evident (Fig. 7, A–C). These results indicate that administration of MB-001 to mice maintained under standard vivarium lighting was sufficient to impact rod-mediated function, likely because of the accumulation of apo-opsin (Lyubarsky et al., 2004) and consequent constitutive signaling that desensitizes the phototransduction pathway in these cells (Cornwall and Fain, 1994; Jäger et al., 1996). To exclude the potential effects of MB-001 on the ERG that are unrelated to visual cycle suppression, we administered MB-001 or vehicle to fully dark-adapted mice for two consecutive days and 2 h after the last dose measured scotopic ERG responses. As shown in Fig. S3, we observed comparable scotopic ERG responses between MB-001– and vehicle-treated mice under

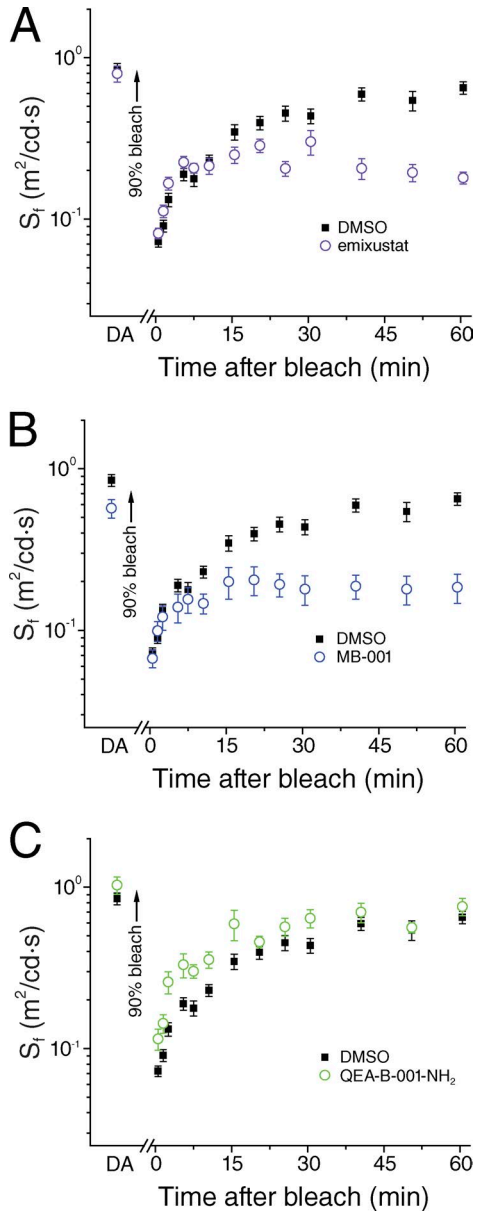

Figure 5. **Effect of RPE65 inhibitors on mouse cone dark adaptation in vivo.** The recovery of cone b-wave flash sensitivity after a 90% bleach was compared between *Gnat1*$^{-/-}$ mice treated with DMSO (n = 16) and mice treated with RPE65 inhibitors. **(A–C)** The late, RPE visual cycle–driven phase of cone dark adaptation was suppressed by emixustat (A; n = 14) and by MB-001 (B; n = 14), but not by QEA-B-001-NH_2 (C; n = 10). The early, retina visual cycle–driven phase of cone dark adaptation was unaffected in all three cases. Data are presented as means ± SEM.

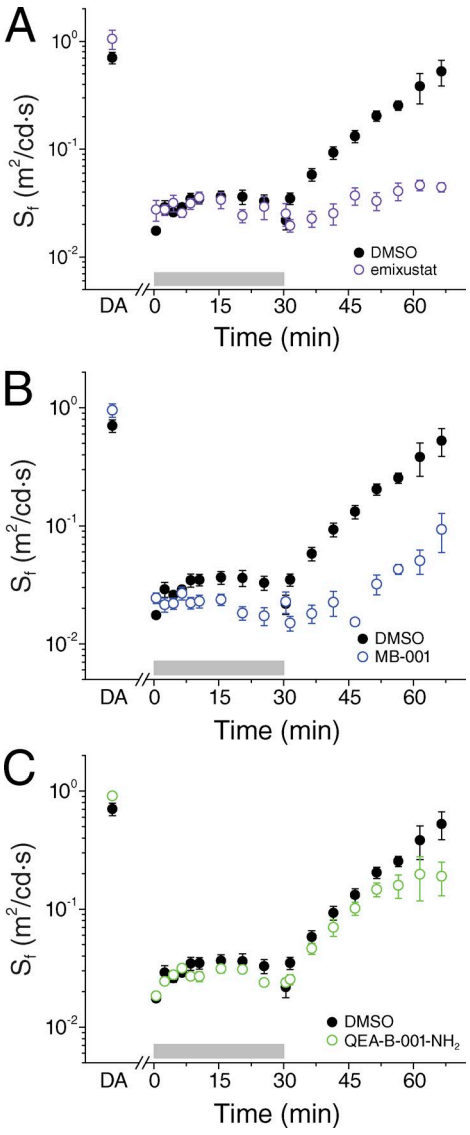

Figure 6. **Effect of RPE65 inhibitors on mouse cone function in vivo during and after prolonged exposure to background light.** Cone b-wave sensitivity was monitored during a 30-min exposure of 3-mo-old *Gnat1*$^{-/-}$ mice to bright 300-cd/m^2 white background light (gray bars) and then for 35 min in darkness. **(A)** Compared with control DMSO treatment (n = 6), cones from mice treated with emixustat (n = 10) were equally desensitized by the background light but had largely suppressed subsequent dark adaptation. **(B)** In contrast, in mice treated with MB-001 (n = 8), cones gradually desensitized during background adaptation and had suppressed subsequent dark adaptation. **(C)** Treatment with QEA-B-001-NH_2 (n = 6) had no effect on the function of cones in background light or during the subsequent dark adaptation. Data are presented as means ± SEM.

these conditions, consistent with the lack of prebleach ERG effects observed in *Gnat1*$^{-/-}$ mice (Figs. 5 B and 6 B). After this initial ERG recording, mice were subjected to a strong photobleach (10 min × 10,000 lux) and then allowed to dark adapt for 22 h. After dark adaptation, we repeated the scotopic ERG measurements. Whereas vehicle-treated mice had postbleach responses comparable to the prebleach values, those from MB-001–treated mice were drastically reduced (Fig. S3). After a 2-wk drug washout period, the responses of the MB-001–treated mice returned to baseline, demonstrating a lack of long-term residual effects caused by either the drug treatment or light exposure. These data confirm that ERG effects arising from MB-001 treatment are a result of visual cycle suppression rather than off-target effects and that this suppression is fully reversible.

Under light-adapted conditions, the mouse ERG response has a major positive b-wave that is preceded by a small negative wave (Fig. 8 A). The positive b-wave reflects cone-depolarizing bipolar cell activity, whereas the negative wave primarily reflects postreceptor activity of the inner retina (Sharma et al., 2005; Shirato

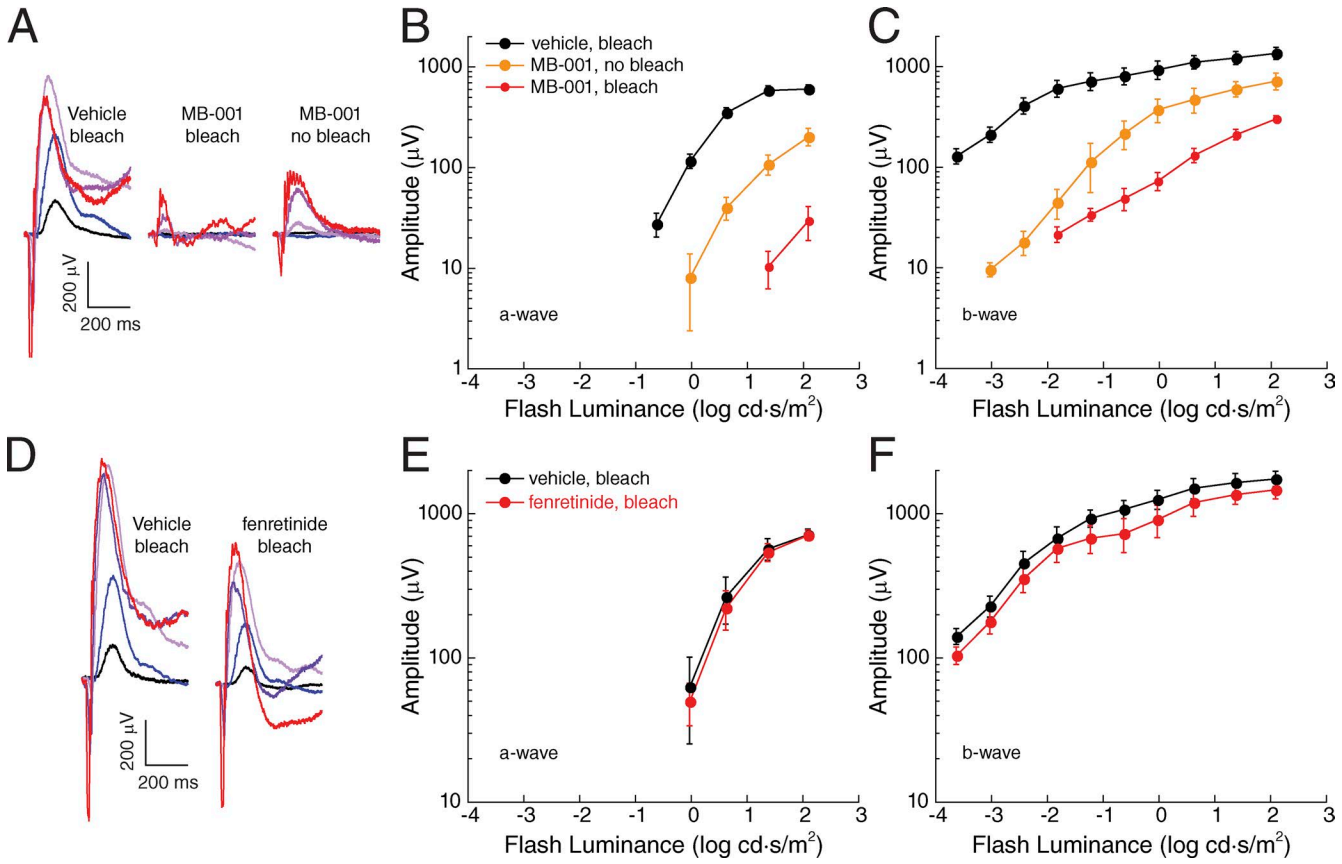

Figure 7. **Impact of MB-001 and fenretinide administration on wild-type mouse scotopic ERG responses. (A)** Representative dark-adapted ERGs obtained from 7-mo-old C57BL/6J mice treated with vehicle and bleached, treated with MB-001 and bleached, or treated with MB-001 and not bleached. Animals were dark adapted for 6 h before ERG recordings. Flash strength is color coded: black, −3.6 log cd·s/m^2; blue, −2.4 log cd·s/m^2; light purple, −1.2 log cd·s/m^2; purple, 0 log cd·s/m^2; red, 1.4 log cd·s/m^2. **(B and C)** Dark-adapted a-wave and b-wave responses for the three treatment groups. Note that MB-001 reduced a- and b-wave ERG amplitude recovery both after a bleach and, to a lesser extent, in mice reared under standard vivarium lighting conditions. Data points indicate means (±SEM) of five mice per group for the vehicle and bleached, MB-001–treated groups and three mice for the nonbleached, MB-001–treated group. **(D)** Representative dark-adapted ERGs obtained from 2-mo-old C57BL/6J mice administered vehicle and bleached or administered fenretinide and bleached. Animals were dark adapted for 6 h before ERG recordings. Flash strength is color coded: black, −3.6 log cd·s/m^2; blue, −2.4 log cd·s/m^2; light purple, −1.2 log cd·s/m^2; purple, 0 log cd·s/m^2; red, 1.4 log cd·s/m^2. **(E and F)** Scotopic a-wave and b-wave responses for the two treatment groups. Data points indicate means (±SEM) of three mice per group. Fenretinide treatment reduced scotopic b-wave amplitudes slightly, whereas a-wave responses were unaffected.

et al., 2008). Light-adapted ERGs of mice administered MB-001 were reduced in both bleached and nonbleached animals in comparison to those treated with vehicle (Fig. 8, A and B). This suppression was most prominent with midintensity flashes where the ERG response was reduced approximately fivefold and threefold in bleached and nonbleached animals, respectively, and gradually equalized with higher flash stimuli. These results indicate that RPE65 plays a role in restoring cone photoreceptor activity in wild-type mice during dark adaptation after a bleach, as well as during exposure to standard vivarium light levels, consistent with the results obtained from *Gnat1*$^{-/-}$ mice.

We also investigated the impact of multiday treatment with the DES1 inhibitor fenretinide on ERG responses in wild-type mice. We administered fenretinide for three consecutive days at a dose of 267 mg/kg/day, which is equivalent to a high-dose regimen previously evaluated for ocular effects in humans (Marmor et al., 2008). On the third day, 1 h after the final injection, we subjected the mice to a 10-min × 10,000-lux photobleach and then allowed them to dark adapt for 6 h before ERG recordings were performed. Based on human clinical data, fenretinide can exert profound effects on rod function with little impact on cones (Marmor et al., 2008). In wild-type C57BL6/J mice, we found that scotopic ERGs were mildly reduced (Fig. 7, D–F), whereas photopic responses were slightly elevated relative to vehicle control (Fig. 8, C and D). Thus, high-dose fenretinide does not appear to negatively impact the steady-state level of cone pigment regeneration to a detectable degree under these conditions.

Effects of multiday RPE65 inhibitor treatment on ground squirrel cone ERG responses

Many of the biochemical studies on the intraretinal visual cycle have been conducted using retinas from cone-dominant species (Mata et al., 2002, 2005; Gollapalli and Rando, 2003; Muniz et al., 2009). However, the contribution of the classical visual cycle to cone function has not been thoroughly evaluated in these animals. We tested the effect of RPE65 inhibition on cone-driven ERG responses in the ground squirrel, a rodent whose photoreceptor population consists almost exclusively of cones (Jacobs

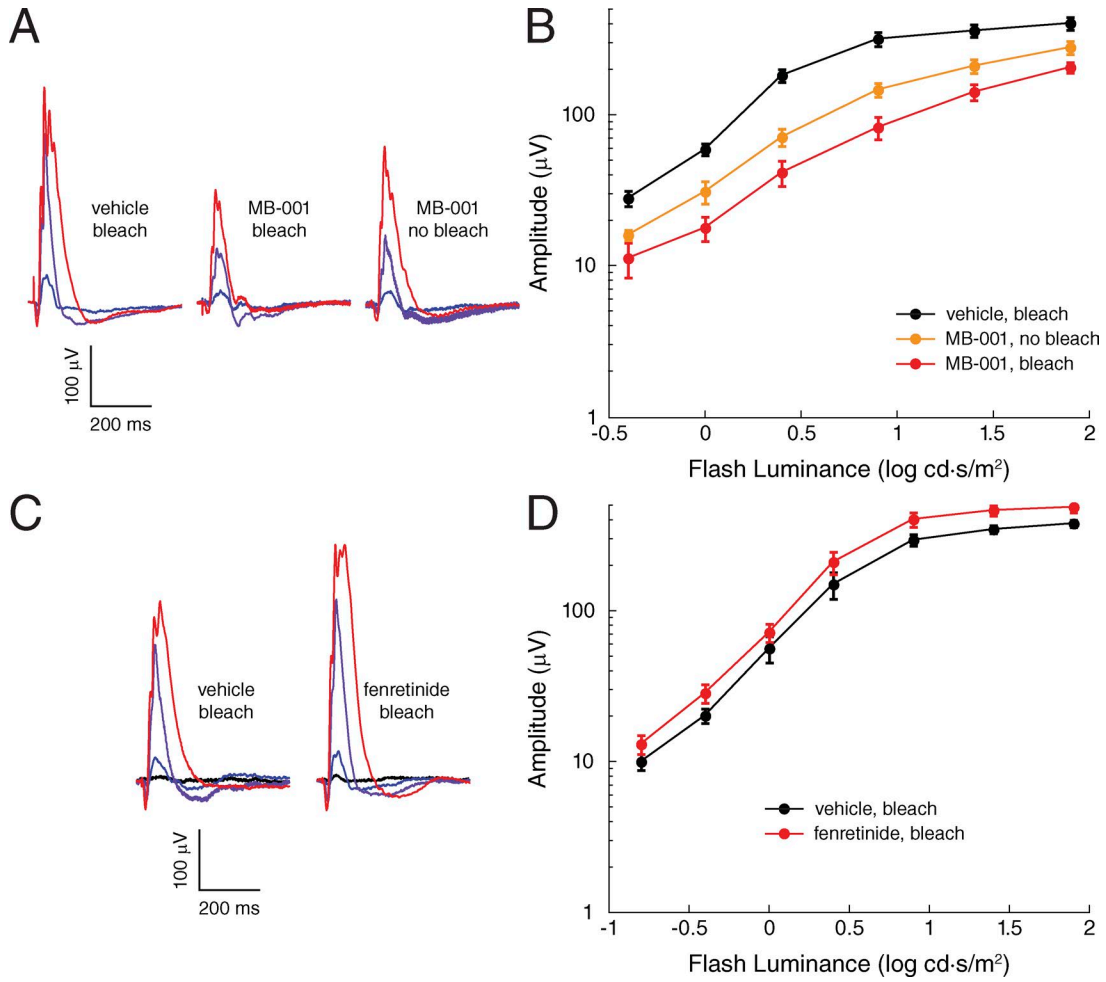

Figure 8. **Impact of MB-001 and fenretinide administration on wild-type mouse cone-driven ERG responses. (A)** Representative light-adapted ERGs obtained from 7-mo-old C57BL/6J mice administered vehicle and bleached, administered MB-001 and bleached, or administered MB-001 and not bleached. These photopic ERGs were recorded immediately after the scotopic recordings shown in Fig. 7 (A–C) and a 5-min light adaptation period under steady 30 cd/m^2 background light, which was maintained during the recordings. Flash strength is color coded: blue, 0 log cd·s/m^2; purple, 0.9 log cd·s/m^2; red, 1.9 log cd·s/m^2. **(B)** Photopic b-wave responses for the three treatment groups. Data points indicate means (±SEM) of five mice per group for the vehicle and MB-001 bleach groups and three mice for the MB-001 no-bleach group. Note that MB-001 reduced cone ERG amplitude recovery after a bleach and reduced cone ERG amplitude to a lesser extent in mice reared under standard vivarium lighting conditions. **(C)** Representative light-adapted ERGs obtained from 2-mo-old C57BL/6J mice administered vehicle and bleached or administered fenretinide and bleached. These photopic ERGs were recorded immediately after the scotopic recordings shown in Fig. 7 (D–F) and a 5-min light adaptation period under steady 30 cd/m^2 background light, which was maintained during the recordings. Flash strength is color coded: black, −0.8 log cd·s/m^2; blue, 0 log cd·s/m^2; purple, 0.9 log cd·s/m^2; red, 1.9 log cd·s/m^2. **(D)** Photopic b-wave responses for the two treatment groups. Data points indicate the means (±SEM) of three mice per group. Note that light-adapted ERG b-wave amplitudes were slightly greater in mice treated with fenretinide as compared with those treated with vehicle.

and Yolton, 1969; Mustafi et al., 2016). MB-001 or vehicle was administered to these animals for three consecutive days. After pupillary dilation, MB-001– or vehicle-treated squirrels were uniocularly exposed to bright light for 10 min, which completely suppressed cone responses to a midintensity flash, followed by ERG recordings from both eyes. After a 6-wk washout period, the treatment and control groups were crossed over and the experiment was repeated. Using this treatment regimen, which caused pronounced ERG effects in mice as described above, the a- and b-wave ERG amplitudes were essentially unaffected by MB-001 treatment in the ground squirrels (Fig. S4). Unlike mice, ground squirrels do not produce a reliable rod ERG response that could be used to definitively assess the degree of RPE65 inhibition by MB-001 (Jacobs et al., 1980). Although MB-001 was detected in the eyes of ground squirrels (Figs. S5 and S6), given the relatively long period of time that elapsed between the final treatment dose and the ERG recordings (~1 d), we considered the possibility that MB-001 is more rapidly eliminated in ground squirrels than in mice and hence lost its efficacy during this period.

To address this possibility, we repeated the experiment but administered the final treatment dose 2 h before ERG recordings. We used the original 8 mg/kg dose as well as an 80 mg/kg dose to help ensure that an adequate concentration of MB-001 was present in the RPE at the time of ERG recording. To directly measure the degree of RPE65 inhibition in these animals, the RPE was collected from squirrel eyes after ERG recordings, and RPE65 activity was measured from the cell lysates. As shown in Fig. 9, 11-cis-retinol was generated in assays using RPE from

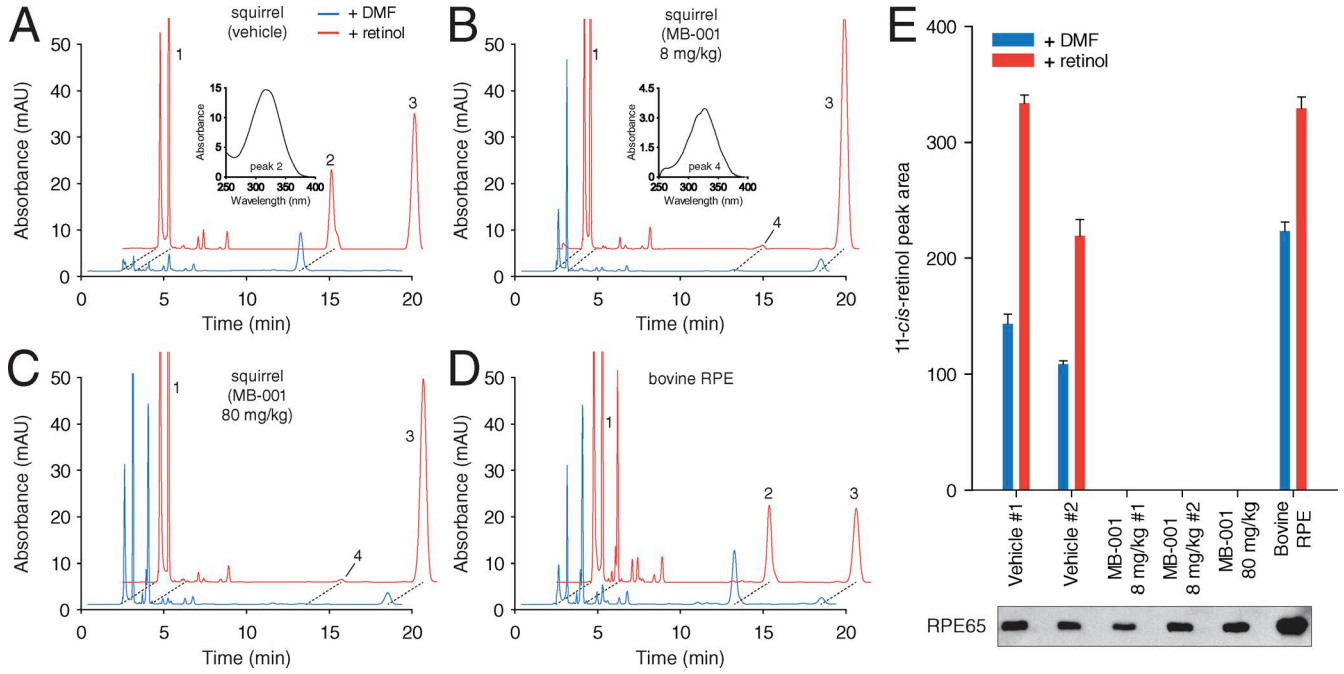

Figure 9. **Impact of MB-001 treatment on the production of 11-cis-retinol by ground squirrel RPE. (A–D)** Examples of high-performance liquid chromatography separation of retinoids obtained from vehicle-treated squirrels (A), squirrels treated with MB-001 at doses of 8 mg/kg/day (B) or 80 mg/kg/day (C), and untreated bovine RPE (D). Blue and red traces show separations from assays performed only with added vehicle (dimethylformamide) or with all-trans-retinol delivered in dimethylformamide, respectively. Retinoids are labeled as follows: 1, all-trans-retinyl esters; 2, 11-cis-retinol; 3, all-trans-retinol; and 4, 13-cis-retinol. The insets in A and B show absorbance spectra for peaks 2 and 3. **(E)** Quantification of 11-cis-retinol production by the indicated RPE samples. The different vehicle and 8 mg/kg MB-001 samples are biological replicates. Each sample was assayed in duplicate. The results are presented as means, and the error bars represent SDs. An RPE65 immunoblot of the samples loaded at the same relative amounts as used in the assay demonstrates that the difference in isomerase activity between the vehicle and drug-treated samples is not attributable to large differences in RPE65 levels. Only a single band at ∼65 kD corresponding to RPE65 was visualized on the immunoblot; hence, the image was cropped to the area surrounding this band. DMF, dimethylformamide.

vehicle-treated animals (Fig. 9 A), and the production was augmented by the addition of all-trans-retinol to the assay mixture, as observed for bovine RPE (Fig. 9 D). In contrast, RPE samples obtained from squirrels treated with either dose of MB-001 failed to generate 11-cis-retinol (Fig. 9, B and C). Immunoblots showed a comparable amount of RPE65 in each sample, thus ruling out a lack of visual cycle enzymes in the MB-001–treated samples underlying the absence of activity (Fig. 9 E). Whereas vehicle and 8 mg/kg/day MB-001 treatment were well tolerated by the animals, significant (>50%) mortality was observed for animals treated with the 80 mg/kg/day dose of MB-001.

We applied two different ERG recording paradigms to these animals. First, we subjected the animals to a 10-min photobleach that completely suppressed ERG responses and then monitored for ERG recovery with midintensity test flashes over the ensuing 10 min. Second, after the 10-min recovery period, we subjected animals to a series of light flashes to assess ERG responses over a range of flash stimuli. Compared with the vehicle treatment, MB-001 at both doses dramatically prolonged the time to recovery in all animals investigated (Fig. 10 and Table 1). The mean time constant for recovery was ∼51 s before treatments and 40 s after 3 d of vehicle treatment but was slowed to ∼1,500 s and ∼294 s in the low and high MB-001 treatment groups. Moreover, in two of the four animals treated with MB-001, the fractional recovery 10 min after the end of the photobleach was substantially less than the pretreatment value, whereas vehicle-treated animals on average matched their pretreatment recovery levels (Fig. 10). Despite this marked delay in ERG response recovery, animals from all treatment groups had only subtle alterations in their ability to respond to subsequent strobe flashes (Fig. 11). Compared with pretreatment responses (Fig. 11 A), the effects of MB-001 treatment at a dose of 8 mg/kg/day were essentially indistinguishable from vehicle alone (Fig. 11, B and C). MB-001 at 80 mg/kg produced varying responses in the two animals treated with this regimen (Fig. 11 D). In one animal, ERG responses were comparable to those of vehicle treatment. The other animal had a much more pronounced response to the drug treatment, with marked effects on pre- and postbleach a-wave and b-wave responses. We note that this animal died 3 d after the recordings were made. It is likely that the more profound effect observed in this animal was a result of toxicity rather than an accentuated on-target effect of the drug.

We also tested the effects of fenretinide on the squirrel cone ERG response. We administered fenretinide at a dose of 166 mg/kg, the body surface area–adjusted equivalent dose used in mice, daily for three consecutive days and then assessed ERG responses using the same experimental protocol described in the preceding paragraph. We found that fenretinide treatment slowed the time constant of recovery about threefold relative to vehicle (Fig. 10 and Table 1) but did not impact responsiveness to a subsequently delivered strobe flash series (Fig. 11 E). We observed a trend toward the extent of recovery being augmented by fenretinide

Table 1. **Rate constants and recoveries derived from curve fitting to the data shown in Fig. 10**

Vehicle				MB001 (8 mg/kg)				MB001 (80 mg/kg)				Fenretinide			
Recovery time constant		Recovery fraction		Recovery time constant		Recovery fraction		Recovery time constant		Recovery fraction		Recovery time constant		Recovery fraction	
Day 1	Day 3	Day 1	Day 3	Day 1	Day 3	Day 1	Day 3	Day 1	Day 3	Day 1	Day 3	Day 1	Day 3	Day 1	Day 3
s				*s*				*s*				*s*			
35.6	44.0	0.7450	0.6400	52.8	2067.7	0.7480	0.4130	47.0	404.6	0.9710	0.5380	44.2	188.9	0.7540	0.9240
32.8	28.0	0.9620	0.7600	32.8	933.1	0.6910	0.6860	14.4	183.5	0.7550	0.6010	107.1	220.4	0.5850	0.6630
77.6	48.2	0.7450	0.8420									48.3	150.9	0.9490	1.2230
48.67	40.07	0.82	0.75	42.80	1500.40	0.72	0.55	30.70	294.05	0.86	0.57	66.53	186.73	0.76	0.94

Recovery fraction indicates the degree of recovery 10 min after the end of the photobleaching period. For each treatment, the individual rows represent values calculated from individual animals. The final row shows column averages.

treatment relative to vehicle control (Fig. 10 and Table 1), which is consistent with our findings in wild-type mice (Fig. 8, C and D).

Collectively, the experiments in ground squirrels indicate that RPE65 is involved in mammalian cone pigment regeneration as deduced from sensitivity recovery measurements after an extended photobleach, but the cones can clearly function in a relatively normal fashion with RPE65 activity acutely blocked by pharmacological means. The same conclusion can be drawn for the putative inhibition of DES1 activity by fenretinide, although the effects of this compound were milder compared with MB-001.

Discussion

The electrophysiological experiments described in this study reveal differing effects of three RPE65-selective inhibitors (Ret-NH_2, emixustat, and MB-001) on cone pigment regeneration and cone photoreceptor dark adaptation.

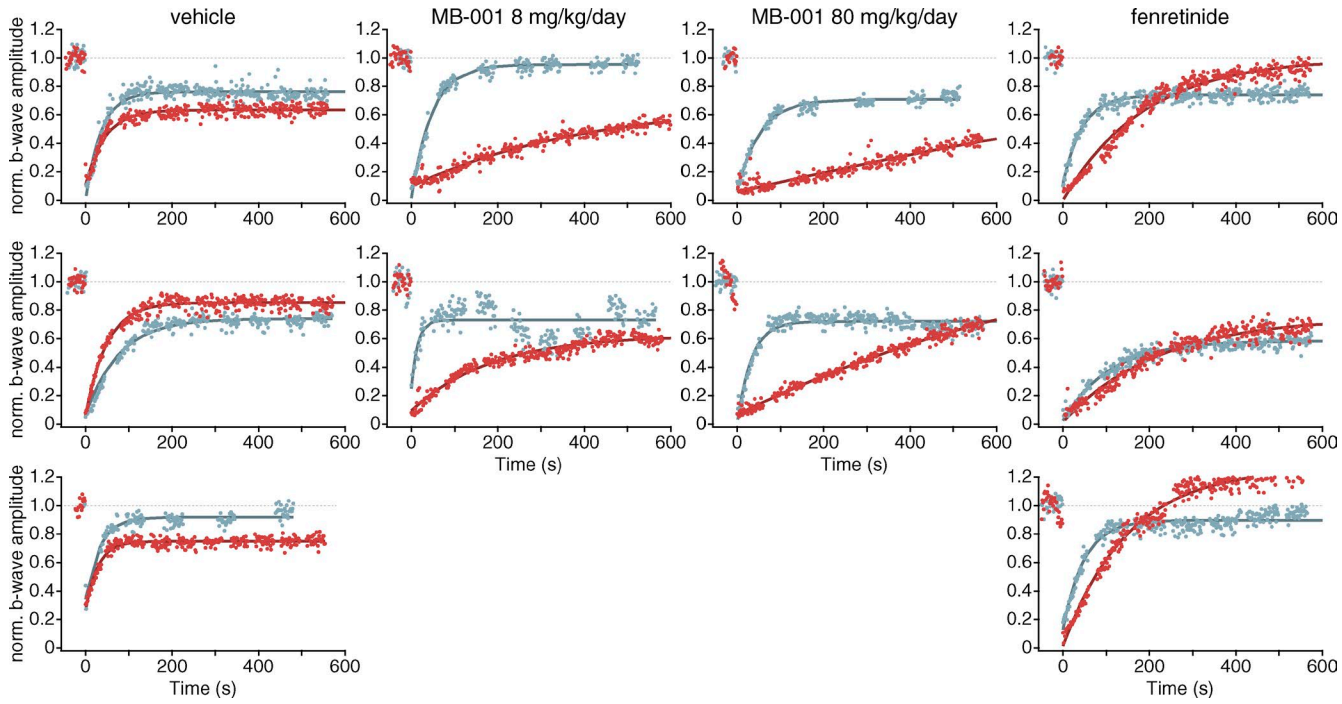

Figure 10. **Recovery of ERG b-wave responses after a photobleach in drug- and vehicle-treated ground squirrels.** After baseline ERG recordings, the animals were subjected to a 10-min photobleach that completely suppressed b-wave responses. They were subsequently monitored for ERG recovery with flashes giving approximately half-maximal responses (100 cd·s/m^2, except for the animal whose responses are shown in the lower graph of the 80 mg/kg/day MB-001 column, which required 300 cd·s/m^2 to elicit midsaturating responses). Data shown as blue circles were obtained at day 1 before drug or vehicle treatment. Data shown as red circles were obtained after three consecutive days of vehicle or drug treatment at the indicated dose. The later ERGs were measured ∼2 h after the final dose of drug. Each panel shows data from a single animal. MB-001 at either dose greatly delays the recovery of cone sensitivity. Fenretinide also delayed, to a smaller degree, cone sensitivity recovery in two of the three treated animals.

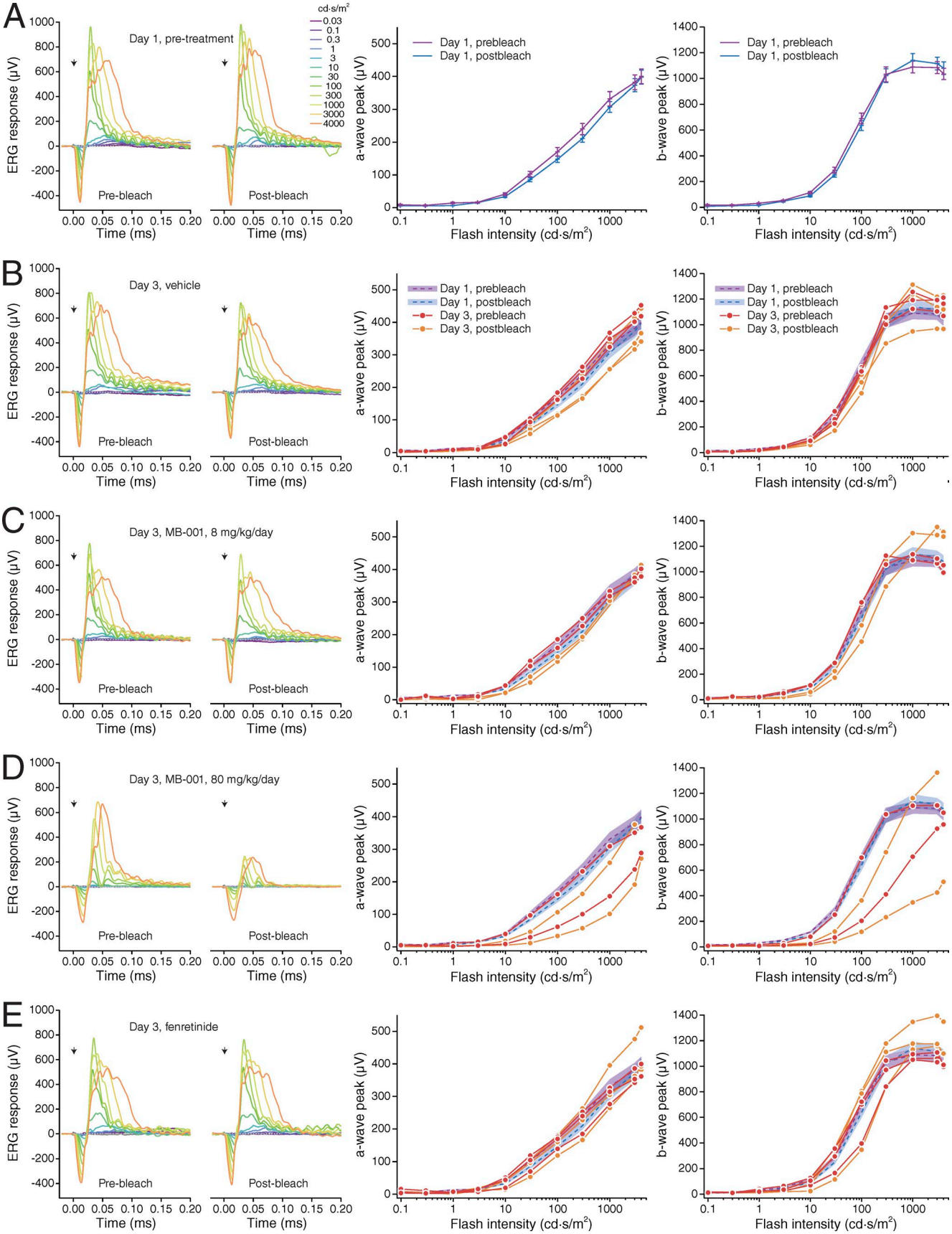
A
Day 1, pre-treatment
cd·s/m²
0.03
0.1
0.3
1
3
10
30
100
300
1000
3000
4000
ERG response (μV)
Pre-bleach
Post-bleach
Time (ms)
Day 1, prebleach
Day 1, postbleach
a-wave peak (μV)
b-wave peak (μV)
Flash intensity (cd·s/m²)
B
Day 3, vehicle
Day 3, prebleach
Day 3, postbleach
C
Day 3, MB-001, 8 mg/kg/day
D
Day 3, MB-001, 80 mg/kg/day
E
Day 3, fenretinide

After brief, intense light exposure, the initial fast recovery of cone light sensitivity, which reflects intraretinal visual cycle function (Kolesnikov et al., 2011), is largely unaffected in *Gnat1*$^{-/-}$ mice treated with RPE65-selective inhibitors, whereas the second phase recovery component that completes dark adaptation and is attributable to the classical visual cycle (Kolesnikov et al., 2015) is markedly slowed (Fig. 3 A and Fig. 5, A and B). These observations are consistent with the existence of a rapid RPE65-independent mechanism of visual chromophore delivery to cone photoreceptors.

The cones of mice treated with RPE65 inhibitors also displayed sustained light responsiveness during prolonged exposure to moderately intense background illumination, again suggesting RPE65-independent chromophore regeneration (Fig. 6, A and B). Interestingly, the time required for cone photoreceptor resensitization after the 30-min light exposure (Fig. 6) was somewhat slower compared with the situation in which bleaching was achieved with a single intense light flash (Fig. 5), possibly reflecting a depletion of cis-retinoid sources. Resensitization was slowed to a much greater degree in mice treated with RPE65 inhibitors, indicating that RPE65 may be particularly important in supporting cone function during sustained light exposure.

Consistent with this proposal, cone ERG responses were also suppressed in wild-type mice after extended administration of MB-001 and a photobleach followed by a dark adaptation period, as indicated by the reduced photopic b-wave amplitudes in these animals compared with vehicle-treated controls (Fig. 8, A and B). We also observed mild suppression of cones and, to a greater degree, rod responses without a prior photobleach when the mice were reared in normal vivarium light. This likely reflects bleaching desensitization caused by the inability of the photoreceptor pigments to regenerate after being bleached by the vivarium light.

In the cone-dominant ground squirrel, as in *Gnat1*$^{-/-}$ mice, the time required for flash sensitivity recovery after an extended bleach was markedly prolonged in MB-001–treated animals, and in some cases the extent of sensitivity recovery was also suppressed (Fig. 10 and Table 1). However, after the recovery period, the ground squirrel cone ERG responses to a flash series were remarkably well preserved (Fig. 11), indicating the presence of robust pigment regeneration mechanism(s) that are not reliant on continuous RPE65 activity. In both wild-type mice and ground squirrels, we conclusively ruled out residual RPE65 activity as being responsible for the cone-mediated responses. In the case of mice, this was confirmed by the absence of rod-related ERG signals after a 6-h postbleach dark adaptation (Fig. 7, A–C). In squirrels, RPE65 activity in isolated RPE was abolished by MB-001 treatment (Fig. 9).

Our finding that cone function is preserved in the setting of reduced RPE-based visual cycle function is consistent with data obtained from human clinical trials of emixustat treatment. Subjects receiving both acute (Kubota et al., 2012) and chronic (Kubota et al., 2014) dosing regimens had minimal changes in cone ERG flash and flicker responses despite substantial suppression of rod responses because of RPE65 blockade. Although overall cone electrical activity was preserved, dyschromatopsia was a frequently reported side effect associated with emixustat treatment, which has been attributed to perturbations in rod cell modulation of cone sensory output (Kubota et al., 2012).

Fenretinide also exerted modulatory effects on ERG responses in these animal models. In isolated *Gnat1*$^{-/-}$ mouse retinas, fenretinide reduced the extent of cone sensitivity recovery (Fig. 4), although not as much as observed after the complete block of the intraretinal visual cycle by ablation of the Müller cells (Wang and Kefalov, 2009). We also observed a lag in ground squirrel cone sensitivity recovery after a bleach in animals treated with this drug (Fig. 10 and Table 1). These effects of fenretinide appear to be dependent on the time allowed for dark recovery, as fenretinide-treated wild-type mice that were allowed an extended time for dark adaptation (6 h) had fully recovered and perhaps even had elevated cone ERG responses (Fig. 8, C and D). We also observed slightly elevated responses after bleach recovery in ground squirrels (Fig. 10 and Table 1). The reduction of cone sensitivity exerted by fenretinide may relate to its ability to inhibit the putative Müller cell retinoid isomerase DES1 (Kaylor et al., 2013). Although fenretinide exhibits selectivity for DES1 over RPE65 (Fig. 2, B and C), it has other documented molecular targets, including LRAT (Dew et al., 1993), β-carotene dioxygenase 1 (Poliakov et al., 2012a), and retinol-binding protein 4 (Berni and Formelli, 1992), all of which are known to contribute directly or indirectly to visual cycle function. Moreover, retinoic acid, a metabolite of fenretinide, can inhibit retinol dehydrogenase enzymes (Law and Rando, 1989), potentially including those relevant to the cone-specific visual cycle (Sato and Kefalov, 2016). Therefore, we cannot rule out that the ERG alterations are caused by fenretinide's effects on enzymes other than DES1. The relatively

Figure 11. **Impact of MB-001 and fenretinide treatment on ground squirrel ERG responses to a range of flash intensities. (A)** Ground squirrel ERG responses to a flash series were measured on day 1 before any drug or vehicle treatment both before and after a 10-min photobleach. **(B–E)** The responses were measured again in the same fashion 3 d later after daily administration of vehicle, MB-001 at 8 mg/kg/day, MB-001 at 80 mg/kg/day, and fenretinide at 166 mg/kg/day. The final dose of drug was administered ∼2 h before the ERG recordings. The left graphs show ERG traces for each type of treatment. The arrows indicate the time of flash onset. The middle panels show a-wave responses to each flash, and the right panels show the corresponding graphs for b-wave responses. The luminance-response plots of A show averaged data for all animals studied (n = 10). The luminance-response plots for B–E show the posttreatment responses for the individual animals studied (red and orange circles for pre- and posttreatment responses, respectively) along with the averaged day 1 responses (mean shown as a dashed line with the SDs shown as shaded error bars). Vehicle-treated group, n = 3; 8 mg/kg MB-001–treated group, n = 2; 80 mg/kg MB-001–treated group, n = 2; fenretinide-treated group, n = 3. Apart from a single animal in the high-dose MB-001 group (D), the pre- and postbleach responses in drug- and vehicle-treated animals were highly similar to the day 1 pretreatment responses. The greater responses in the single animal may have been caused by off-target drug toxicity.

subtle effects of fenretinide on cone function are in line with clinical data showing that this compound has little impact on human cone function, even at high doses (Kaiser-Kupfer et al., 1986; Marmor et al., 2008).

Collectively, these data demonstrate that cones rely on both continuous RPE65 activity and an independent second source of 11-cis-retinaldehyde for regeneration of their visual pigments. The reduced ERG recovery rate that we observe in mice treated with RPE65 inhibitors when cone bleaching is achieved with a prolonged light exposure rather than a short step of light suggests a critical role for stored forms of 11-cis-retinoids in cone pigment regeneration. Indeed, the involvement of cellular 11-cis-retinaldehyde–binding protein (CRALBP) in cone pigment regeneration has received considerable experimental support (Saari et al., 2001; Collery et al., 2008; Fleisch et al., 2008; Xue et al., 2015). CRALBP is expressed in the RPE and Müller glia (Bunt-Milam and Saari, 1983), where it noncovalently binds 11-cis-retinaldehyde as well as 11-cis-retinol with low nanomolar affinity (Saari et al., 1982; Saari and Bredberg, 1987; Crabb et al., 1998). These cis-retinoids can be released for rapid visual pigment regeneration (Saari and Crabb, 2005). In CRALBP knockout (*Rlbp1*$^{-/-}$) mice, rod dark adaptation after illumination is delayed >10-fold (Saari et al., 2001). *Rlbp1*$^{-/-}$ mice also exhibit defects in M-opsin cellular distribution and consequently display M-cone dysfunction because of cis-retinoid deficiency, including greatly suppressed M-cone sensitivity and dark adaptation. These abnormalities can be rescued by selective reexpression of CRALBP in Müller glia (Xue et al., 2015).

The contribution of CRALBP toward intraretinal cone regeneration can be estimated. The quantity of this protein in the bovine neurosensory retina is ∼1 nmol/eye, and its molar ratio to rhodopsin is 1:20 (Stubbs et al., 1979). Assuming that (a) this ratio is similar in the mouse retina, (b) the amount of cone opsin in mouse retina is ∼1% of rhodopsin (Daniele et al., 2011), and (c) CRALBP and 11-cis-retinoids form a 1:1 complex (Saari et al., 1982; He et al., 2009), we can estimate that there are on the order of five CRALBP-associated 11-cis-retinoids per cone pigment stored in Müller cells.

Adding to this source of potential chromophore for the regeneration of cone pigments are 11-cis-retinyl esters found in variable amounts in the RPE and neurosensory retina, depending on the species (Bridges et al., 1987; Rodriguez and Tsin, 1989; Das et al., 1992; Kaylor et al., 2013; Palczewska et al., 2014; Babino et al., 2015; Mustafi et al., 2016). Ground squirrels in particular possess large quantities of 11-cis-retinyl esters in their neural retina (Mata et al., 2002), and this may account for the highly resilient responsiveness of their cones.

The availability of these stored forms of readily mobilized 11-cis-retinoids, together with the ability of cones to operate over a wide dynamic range and with high degrees of baseline bleaching (Malchow and Yazulla, 1986; Jones et al., 1993), could explain the ability of these cells to maintain function in sustained bright light. Two important outstanding issues are the origin of 11-cis-retinoids stored in the neural retina (i.e., derived from the classical vs. intraretinal visual cycle) and the necessity for ongoing cis-retinoid production by the putative intraretinal visual cycle for cone-mediated vision.

Acknowledgments

We thank Dr. Leslie T. Webster Jr. and members of the Palczewski laboratory for helpful comments on this manuscript and Dr. Jianying Kiser for technical assistance.

This work was supported by the National Institutes of Health (R01EY009339 to K. Palczewski and P.D. Kiser, R24EY024864 and R24EY027283 to K. Palczewski, R01EY019312 to V.J. Kefalov, R01EY021126 to K. Palczewski and V.J. Kefalov, R01CA157735 to G.P. Tochtrop, P30EY011373 to the Department of Ophthalmology and Visual Sciences at Case Western Reserve University, P30EY025585 to the Cleveland Clinic Cole Eye Institute, and P30EY002687 to the Department of Ophthalmology and Visual Sciences at Washington University and the National Eye Institute Intramural Research Program to W. Li); the U.S. Department of Veterans Affairs (IK2BX002683 to P.D. Kiser and a Research Career Scientist Award to N.S. Peachey); the Foundation Fighting Blindness (supporting K. Palczewski); the National Science Foundation (MCB-084480 to G.P. Tochtrop); and Research to Prevent Blindness. K. Palczewski is John H. Hord Professor of Pharmacology.

The authors declare no competing financial interests.

Author contributions: Experiments were conceived and designed by P.D. Kiser, G.P. Tochtrop, W. Li, N.S. Peachey, V.J. Kefalov, and K. Palczewski. Data acquisition, analysis, and interpretation were performed by P.D. Kiser, J. Zhang, A. Sharma, J.M. Angueyra, A.V. Kolesnikov, M. Badiee, J. Kinoshita, N.S. Peachey, and V.J. Kefalov. Drafting and revising the manuscript were done by P.D. Kiser, J. Zhang, J.M. Angueyra, A.V. Kolesnikov, M. Badiee, J. Kinoshita, N.S. Peachey, V.J. Kefalov, and K. Palczewski. All authors have approved the final version of the manuscript.

Edward N. Pugh served as guest editor.

Submitted: 20 April 2017
Revised: 18 December 2017
Accepted: 22 January 2018

References

Abd-El-Barr, M.M., M.E. Pennesi, S.M. Saszik, A.J. Barrow, J. Lem, D.E. Bramblett, D.L. Paul, L.J. Frishman, and S.M. Wu. 2009. Genetic dissection of rod and cone pathways in the dark-adapted mouse retina. *J. Neurophysiol.* 102:1945–1955. https://doi.org/10.1152/jn.00142.2009

Acland, G.M., G.D. Aguirre, J. Bennett, T.S. Aleman, A.V. Cideciyan, J. Bennicelli, N.S. Dejneka, S.E. Pearce-Kelling, A.M. Maguire, K. Palczewski, et al. 2005. Long-term restoration of rod and cone vision by single dose rAAV-mediated gene transfer to the retina in a canine model of childhood blindness. *Mol. Ther.* 12:1072–1082. https://doi.org/10.1016/j.ymthe.2005.08.008

Albalat, R. 2012. Evolution of the genetic machinery of the visual cycle: a novelty of the vertebrate eye? *Mol. Biol. Evol.* 29:1461–1469. https://doi.org/10.1093/molbev/msr313

Babino, D., B.D. Perkins, A. Kindermann, V. Oberhauser, and J. von Lintig. 2015. The role of 11-cis-retinyl esters in vertebrate cone vision. *FASEB J.* 29:216–226. https://doi.org/10.1096/fj.14-261693

Batten, M.L., Y. Imanishi, T. Maeda, D.C. Tu, A.R. Moise, D. Bronson, D. Possin, R.N. Van Gelder, W. Baehr, and K. Palczewski. 2004. Lecithin-retinol acyltransferase is essential for accumulation of all-trans-retinyl esters in the eye and in the liver. *J. Biol. Chem.* 279:10422–10432. https://doi.org/10.1074/jbc.M312410200

Bavik, C., S.H. Henry, Y. Zhang, K. Mitts, T. McGinn, E. Budzynski, A. Pashko, K.L. Lieu, S. Zhong, B. Blumberg, et al. 2015. Visual cycle modulation as an approach toward preservation of retinal integrity. *PLoS One.* 10:e0124940. https://doi.org/10.1371/journal.pone.0124940

Berni, R., and F. Formelli. 1992. In vitro interaction of fenretinide with plasma retinol-binding protein and its functional consequences. *FEBS Lett.* 308:43–45. https://doi.org/10.1016/0014-5793(92)81046-O

Bridges, C.D., R.A. Alvarez, S.L. Fong, G.I. Liou, and R.J. Ulshafer. 1987. Rhodopsin, vitamin A, and interstitial retinol-binding protein in the rd chicken. *Invest. Ophthalmol. Vis. Sci.* 28:613–617.

Bunt-Milam, A.H., and J.C. Saari. 1983. Immunocytochemical localization of two retinoid-binding proteins in vertebrate retina. *J. Cell Biol.* 97:703–712. https://doi.org/10.1083/jcb.97.3.703

Calvert, P.D., N.V. Krasnoperova, A.L. Lyubarsky, T. Isayama, M. Nicoló, B. Kosaras, G. Wong, K.S. Gannon, R.F. Margolskee, R.L. Sidman, et al. 2000. Phototransduction in transgenic mice after targeted deletion of the rod transducin alpha -subunit. *Proc. Natl. Acad. Sci. USA.* 97:13913–13918. https://doi.org/10.1073/pnas.250478897

Cideciyan, A.V. 2010. Leber congenital amaurosis due to RPE65 mutations and its treatment with gene therapy. *Prog. Retin. Eye Res.* 29:398–427. https://doi.org/10.1016/j.preteyeres.2010.04.002

Collery, R., S. McLoughlin, V. Vendrell, J. Finnegan, J.W. Crabb, J.C. Saari, and B.N. Kennedy. 2008. Duplication and divergence of zebrafish CRALBP genes uncovers novel role for RPE- and Muller-CRALBP in cone vision. *Invest. Ophthalmol. Vis. Sci.* 49:3812–3820. https://doi.org/10.1167/iovs.08-1957

Cornwall, M.C., and G.L. Fain. 1994. Bleached pigment activates transduction in isolated rods of the salamander retina. *J. Physiol.* 480:261–279. https://doi.org/10.1113/jphysiol.1994.sp020358

Crabb, J.W., Z. Nie, Y. Chen, J.D. Hulmes, K.A. West, J.T. Kapron, S.E. Ruuska, N. Noy, and J.C. Saari. 1998. Cellular retinaldehyde-binding protein ligand interactions. Gln-210 and Lys-221 are in the retinoid binding pocket. *J. Biol. Chem.* 273:20712–20720. https://doi.org/10.1074/jbc.273.33.20712

Daniele, L.L., C. Insinna, R. Chance, J. Wang, S.S. Nikonov, and E.N. Pugh Jr. 2011. A mouse M-opsin monochromat: retinal cone photoreceptors have increased M-opsin expression when S-opsin is knocked out. *Vision Res.* 51:447–458. https://doi.org/10.1016/j.visres.2010.12.017

Das, S.R., N. Bhardwaj, H. Kjeldbye, and P. Gouras. 1992. Muller cells of chicken retina synthesize 11-cis-retinol. *Biochem. J.* 285:907–913. https://doi.org/10.1042/bj2850907

Dew, S.E., S.A. Wardlaw, and D.E. Ong. 1993. Effects of pharmacological retinoids on several vitamin A-metabolizing enzymes. *Cancer Res.* 53:2965–2969.

Feathers, K.L., A.L. Lyubarsky, N.W. Khan, K. Teofilo, A. Swaroop, D.S. Williams, E.N. Pugh Jr., and D.A. Thompson. 2008. Nrl-knockout mice deficient in Rpe65 fail to synthesize 11-cis retinal and cone outer segments. *Invest. Ophthalmol. Vis. Sci.* 49:1126–1135. https://doi.org/10.1167/iovs.07-1234

Fleisch, V.C., H.B. Schonthaler, J. von Lintig, and S.C. Neuhauss. 2008. Subfunctionalization of a retinoid-binding protein provides evidence for two parallel visual cycles in the cone-dominant zebrafish retina. *J. Neurosci.* 28:8208–8216. https://doi.org/10.1523/JNEUROSCI.2367-08.2008

Golczak, M., Y. Imanishi, V. Kuksa, T. Maeda, R. Kubota, and K. Palczewski. 2005a. Lecithin:retinol acyltransferase is responsible for amidation of retinylamine, a potent inhibitor of the retinoid cycle. *J. Biol. Chem.* 280:42263–42273. https://doi.org/10.1074/jbc.M509351200

Golczak, M., V. Kuksa, T. Maeda, A.R. Moise, and K. Palczewski. 2005b. Positively charged retinoids are potent and selective inhibitors of the trans-cis isomerization in the retinoid (visual) cycle. *Proc. Natl. Acad. Sci. USA.* 102:8162–8167. https://doi.org/10.1073/pnas.0503318102

Golczak, M., A. Maeda, G. Bereta, T. Maeda, P.D. Kiser, S. Hunzelmann, J. von Lintig, W.S. Blaner, and K. Palczewski. 2008. Metabolic basis of visual cycle inhibition by retinoid and nonretinoid compounds in the vertebrate retina. *J. Biol. Chem.* 283:9543–9554. https://doi.org/10.1074/jbc.M708982200

Golczak, M., P.D. Kiser, D.T. Lodowski, A. Maeda, and K. Palczewski. 2010. Importance of membrane structural integrity for RPE65 retinoid isomerization activity. *J. Biol. Chem.* 285:9667–9682. https://doi.org/10.1074/jbc.M109.063941

Gollapalli, D.R., and R.R. Rando. 2003. Molecular logic of 11-cis-retinoid biosynthesis in a cone-dominated species. *Biochemistry.* 42:14921–14929. https://doi.org/10.1021/bi0356505

He, X., J. Lobsiger, and A. Stocker. 2009. Bothnia dystrophy is caused by domino-like rearrangements in cellular retinaldehyde-binding protein mutant R234W. *Proc. Natl. Acad. Sci. USA.* 106:18545–18550. https://doi.org/10.1073/pnas.0907454106

Jacobs, G.H., and R.L. Yolton. 1969. Dichromacy in the ground squirrel. *Nature.* 223:414–415. https://doi.org/10.1038/223414a0

Jacobs, G.H., R.B.H. Tootell, S.K. Fisher, and D.H. Anderson. 1980. Rod photoreceptors and scotopic vision in ground aquirrels. *J. Comp. Neurol.* 189:113–125. https://doi.org/10.1002/cne.901890107

Jacobson, S.G., T.S. Aleman, A.V. Cideciyan, E. Heon, M. Golczak, W.A. Beltran, A. Sumaroka, S.B. Schwartz, A.J. Roman, E.A. Windsor, et al. 2007. Human cone photoreceptor dependence on RPE65 isomerase. *Proc. Natl. Acad. Sci. USA.* 104:15123–15128. https://doi.org/10.1073/pnas.0706367104

Jacobson, S.G., T.S. Aleman, A.V. Cideciyan, A.J. Roman, A. Sumaroka, E.A. Windsor, S.B. Schwartz, E. Heon, and E.M. Stone. 2009. Defining the residual vision in leber congenital amaurosis caused by RPE65 mutations. *Invest. Ophthalmol. Vis. Sci.* 50:2368–2375. https://doi.org/10.1167/iovs.08-2696

Jäger, S., K. Palczewski, and K.P. Hofmann. 1996. Opsin/all-trans-retinal complex activates transducin by different mechanisms than photolyzed rhodopsin. *Biochemistry.* 35:2901–2908. https://doi.org/10.1021/bi9524068

Jones, G.J., R.K. Crouch, B. Wiggert, M.C. Cornwall, and G.J. Chader. 1989. Retinoid requirements for recovery of sensitivity after visual-pigment bleaching in isolated photoreceptors. *Proc. Natl. Acad. Sci. USA.* 86:9606–9610. https://doi.org/10.1073/pnas.86.23.9606

Jones, G.J., A. Fein, E.F. MacNichol Jr., and M.C. Cornwall. 1993. Visual pigment bleaching in isolated salamander retinal cones. Microspectrophotometry and light adaptation. *J. Gen. Physiol.* 102:483–502. https://doi.org/10.1085/jgp.102.3.483

Kaiser-Kupfer, M.I., G.L. Peck, R.C. Caruso, M.J. Jaffe, J.J. DiGiovanna, and E.G. Gross. 1986. Abnormal retinal function associated with fenretinide, a synthetic retinoid. *Arch. Ophthalmol.* 104:69–70. https://doi.org/10.1001/archopht.1986.01050130079024

Kaylor, J.J., Q. Yuan, J. Cook, S. Sarfare, J. Makshanoff, A. Miu, A. Kim, P. Kim, S. Habib, C.N. Roybal, et al. 2013. Identification of DES1 as a vitamin A isomerase in Müller glial cells of the retina. *Nat. Chem. Biol.* 9:30–36. https://doi.org/10.1038/nchembio.1114

Kaylor, J.J., T. Xu, N.T. Ingram, A. Tsan, H. Hakobyan, G.L. Fain, and G.H. Travis. 2017. Blue light regenerates functional visual pigments in mammals through a retinyl-phospholipid intermediate. *Nat. Commun.* 8:16. https://doi.org/10.1038/s41467-017-00018-4

Kefalov, V.J., M.E. Estevez, M. Kono, P.W. Goletz, R.K. Crouch, M.C. Cornwall, and K.W. Yau. 2005. Breaking the covalent bond--a pigment property that contributes to desensitization in cones. *Neuron.* 46:879–890. https://doi.org/10.1016/j.neuron.2005.05.009

Kiser, P.D., M. Golczak, and K. Palczewski. 2014. Chemistry of the retinoid (visual) cycle. *Chem. Rev.* 114:194–232. https://doi.org/10.1021/cr400107q

Kiser, P.D., J. Zhang, M. Badiee, Q. Li, W. Shi, X. Sui, M. Golczak, G.P. Tochtrop, and K. Palczewski. 2015. Catalytic mechanism of a retinoid isomerase essential for vertebrate vision. *Nat. Chem. Biol.* 11:409–415. https://doi.org/10.1038/nchembio.1799

Kolesnikov, A.V., P.H. Tang, R.O. Parker, R.K. Crouch, and V.J. Kefalov. 2011. The mammalian cone visual cycle promotes rapid M/L-cone pigment regeneration independently of the interphotoreceptor retinoid-binding protein. *J. Neurosci.* 31:7900–7909. https://doi.org/10.1523/JNEUROSCI.0438-11.2011

Kolesnikov, A.V., A. Maeda, P.H. Tang, Y. Imanishi, K. Palczewski, and V.J. Kefalov. 2015. Retinol dehydrogenase 8 and ATP-binding cassette transporter 4 modulate dark adaptation of M-cones in mammalian retina. *J. Physiol.* 593:4923–4941. https://doi.org/10.1113/JP271285

Kubota, R., N.L. Boman, R. David, S. Mallikaarjun, S. Patil, and D. Birch. 2012. Safety and effect on rod function of ACU-4429, a novel small-molecule visual cycle modulator. *Retina.* 32:183–188. https://doi.org/10.1097/IAE.0b013e318217369e

Kubota, R., S. Al-Fayoumi, S. Mallikaarjun, S. Patil, C. Bavik, and J.W. Chandler. 2014. Phase 1, dose-ranging study of emixustat hydrochloride (ACU-4429), a novel visual cycle modulator, in healthy volunteers. *Retina.* 34:603–609. https://doi.org/10.1097/01.iae.0000434565.80060.f8

Kuhne, W. 1878. On the Photochemistry of the Retina and on Visual Purple. Cambridge University Press, Cambridge, UK. 104 pp.

Kusakabe, T., R. Kusakabe, I. Kawakami, Y. Satou, N. Satoh, and M. Tsuda. 2001. Ci-opsin1, a vertebrate-type opsin gene, expressed in the larval ocellus of the ascidian Ciona intestinalis. *FEBS Lett.* 506:69–72. https://doi.org/10.1016/S0014-5793(01)02877-0

Lamb, T.D. 2013. Evolution of phototransduction, vertebrate photoreceptors and retina. *Prog. Retin. Eye Res.* 36:52–119. https://doi.org/10.1016/j.preteyeres.2013.06.001

Law, W.C., and R.R. Rando. 1989. The molecular basis of retinoic acid induced night blindness. *Biochem. Biophys. Res. Commun.* 161:825–829. https://doi.org/10.1016/0006-291X(89)92674-0

Lyubarsky, A.L., L.L. Daniele, and E.N. Pugh Jr. 2004. From candelas to photoisomerizations in the mouse eye by rhodopsin bleaching in situ and the light-rearing dependence of the major components of the mouse ERG. *Vision Res.* 44:3235–3251. https://doi.org/10.1016/j.visres.2004.09.019

Lyubarsky, A.L., A.B. Savchenko, S.B. Morocco, L.L. Daniele, T.M. Redmond, and E.N. Pugh Jr. 2005. Mole quantity of RPE65 and its productivity in the generation of 11-cis-retinal from retinyl esters in the living mouse eye. *Biochemistry.* 44:9880–9888. https://doi.org/10.1021/bi0505363

Maeda, T., A.V. Cideciyan, A. Maeda, M. Golczak, T.S. Aleman, S.G. Jacobson, and K. Palczewski. 2009. Loss of cone photoreceptors caused by chromophore depletion is partially prevented by the artificial chromophore pro-drug, 9-cis-retinyl acetate. *Hum. Mol. Genet.* 18:2277–2287. https://doi.org/10.1093/hmg/ddp163

Mahroo, O.A., and T.D. Lamb. 2004. Recovery of the human photopic electroretinogram after bleaching exposures: estimation of pigment regeneration kinetics. *J. Physiol.* 554:417–437. https://doi.org/10.1113/jphysiol.2003.051250

Malchow, R.P., and S. Yazulla. 1986. Separation and light adaptation of rod and cone signals in the retina of the goldfish. *Vision Res.* 26:1655–1666. https://doi.org/10.1016/0042-6989(86)90053-2

Mandal, M.N., G.P. Moiseyev, M.H. Elliott, A. Kasus-Jacobi, X. Li, H. Chen, L. Zheng, O. Nikolaeva, R.A. Floyd, J.X. Ma, and R.E. Anderson. 2011. Alpha-phenyl-N-tert-butylnitrone (PBN) prevents light-induced degeneration of the retina by inhibiting RPE65 protein isomerohydrolase activity. *J. Biol. Chem.* 286:32491–32501. https://doi.org/10.1074/jbc.M111.255877

Marmor, M.F., A. Jain, and D. Moshfeghi. 2008. Total rod ERG suppression with high dose compassionate Fenretinide usage. *Doc. Ophthalmol.* 117:257–261. https://doi.org/10.1007/s10633-008-9132-y

Mata, N.L., R.A. Radu, R.C. Clemmons, and G.H. Travis. 2002. Isomerization and oxidation of vitamin a in cone-dominant retinas: a novel pathway for visual-pigment regeneration in daylight. *Neuron.* 36:69–80. https://doi.org/10.1016/S0896-6273(02)00912-1

Mata, N.L., A. Ruiz, R.A. Radu, T.V. Bui, and G.H. Travis. 2005. Chicken retinas contain a retinoid isomerase activity that catalyzes the direct conversion of all-trans-retinol to 11-cis-retinol. *Biochemistry.* 44:11715–11721. https://doi.org/10.1021/bi050942m

McBee, J.K., V. Kuksa, R. Alvarez, A.R. de Lera, O. Prezhdo, F. Haeseleer, I. Sokal, and K. Palczewski. 2000. Isomerization of all-trans-retinol to cis-retinols in bovine retinal pigment epithelial cells: dependence on the specificity of retinoid-binding proteins. *Biochemistry.* 39:11370–11380. https://doi.org/10.1021/bi001061c

Moiseyev, G., Y. Takahashi, Y. Chen, S. Kim, and J.X. Ma. 2008. RPE65 from cone-dominant chicken is a more efficient isomerohydrolase compared with that from rod-dominant species. *J. Biol. Chem.* 283:8110–8117. https://doi.org/10.1074/jbc.M703654200

Muniz, A., B.S. Betts, A.R. Trevino, K. Buddavarapu, R. Roman, J.X. Ma, and A.T. Tsin. 2009. Evidence for two retinoid cycles in the cone-dominated chicken eye. *Biochemistry.* 48:6854–6863. https://doi.org/10.1021/bi9002937

Mustafi, D., B.M. Kevany, X. Bai, M. Golczak, M.D. Adams, A. Wynshaw-Boris, and K. Palczewski. 2016. Transcriptome analysis reveals rod/cone photoreceptor specific signatures across mammalian retinas. *Hum. Mol. Genet.* 25:4376–4388.

Niccoli, M.2018. MathWorks. Perceptually improved colormaps. Version 1.22 (5.56 MB) by Matteo Niccoli. 7 perceptual colormaps with rainbow-like colors and 1 with heat colors. Available at: https://www.mathworks.com/matlabcentral/fileexchange/28982-perceptually-improved-colormaps (accessed February 1, 2017).

Nikonov, S.S., R. Kholodenko, J. Lem, and E.N. Pugh Jr. 2006. Physiological features of the S- and M-cone photoreceptors of wild-type mice from single-cell recordings. *J. Gen. Physiol.* 127:359–374. https://doi.org/10.1085/jgp.200609490

Nymark, S., H. Heikkinen, C. Haldin, K. Donner, and A. Koskelainen. 2005. Light responses and light adaptation in rat retinal rods at different temperatures. *J. Physiol.* 567:923–938. https://doi.org/10.1113/jphysiol.2005.090662

Palczewska, G., M. Golczak, D.R. Williams, J.J. Hunter, and K. Palczewski. 2014. Endogenous fluorophores enable two-photon imaging of the primate eye. *Invest. Ophthalmol. Vis. Sci.* 55:4438–4447. https://doi.org/10.1167/iovs.14-14395

Palczewski, K. 2006. G protein-coupled receptor rhodopsin. *Annu. Rev. Biochem.* 75:743–767. https://doi.org/10.1146/annurev.biochem.75.103004.142743

Poliakov, E., T. Parikh, M. Ayele, S. Kuo, P. Chander, S. Gentleman, and T.M. Redmond. 2011. Aromatic lipophilic spin traps effectively inhibit RPE65 isomerohydrolase activity. *Biochemistry.* 50:6739–6741. https://doi.org/10.1021/bi200532m

Poliakov, E., A. Gubin, J. Laird, S. Gentleman, R.G. Salomon, and T.M. Redmond. 2012a. The mechanism of fenretinide (4-HPR) inhibition of β-carotene monooxygenase 1. New suspect for the visual side effects of fenretinide. *Adv. Exp. Med. Biol.* 723:167–174. https://doi.org/10.1007/978-1-4614-0631-0_23

Poliakov, E., A.N. Gubin, O. Stearn, Y. Li, M.M. Campos, S. Gentleman, I.B. Rogozin, and T.M. Redmond. 2012b. Origin and evolution of retinoid isomerization machinery in vertebrate visual cycle: hint from jawless vertebrates. *PLoS One.* 7:e49975. https://doi.org/10.1371/journal.pone.0049975

Rahmaniyan, M., R.W. Curley Jr., L.M. Obeid, Y.A. Hannun, and J.M. Kraveka. 2011. Identification of dihydroceramide desaturase as a direct in vitro target for fenretinide. *J. Biol. Chem.* 286:24754–24764. https://doi.org/10.1074/jbc.M111.250779

Redmond, T.M., S. Yu, E. Lee, D. Bok, D. Hamasaki, N. Chen, P. Goletz, J.X. Ma, R.K. Crouch, and K. Pfeifer. 1998. Rpe65 is necessary for production of 11-cis-vitamin A in the retinal visual cycle. *Nat. Genet.* 20:344–351. https://doi.org/10.1038/3813

Rodriguez, K.A., and A.T. Tsin. 1989. Retinyl esters in the vertebrate neuroretina. *Am. J. Physiol.* 256:R255–R258.

Saari, J.C. 2012. Vitamin A metabolism in rod and cone visual cycles. *Annu. Rev. Nutr.* 32:125–145. https://doi.org/10.1146/annurev-nutr-071811-150748

Saari, J.C., and D.L. Bredberg. 1987. Photochemistry and stereoselectivity of cellular retinaldehyde-binding protein from bovine retina. *J. Biol. Chem.* 262:7618–7622.

Saari, J.C., and D.L. Bredberg. 1989. Lecithin:retinol acyltransferase in retinal pigment epithelial microsomes. *J. Biol. Chem.* 264:8636–8640.

Saari, J.C., and J.W. Crabb. 2005. Focus on molecules: cellular retinaldehyde-binding protein (CRALBP). *Exp. Eye Res.* 81:245–246. https://doi.org/10.1016/j.exer.2005.06.015

Saari, J.C., L. Bredberg, and G.G. Garwin. 1982. Identification of the endogenous retinoids associated with three cellular retinoid-binding proteins from bovine retina and retinal pigment epithelium. *J. Biol. Chem.* 257:13329–13333.

Saari, J.C., M. Nawrot, B.N. Kennedy, G.G. Garwin, J.B. Hurley, J. Huang, D.E. Possin, and J.W. Crabb. 2001. Visual cycle impairment in cellular retinaldehyde binding protein (CRALBP) knockout mice results in delayed dark adaptation. *Neuron.* 29:739–748. https://doi.org/10.1016/S0896-6273(01)00248-3

Sato, S., and V.J. Kefalov. 2016. cis Retinol oxidation regulates photoreceptor access to the retina visual cycle and cone pigment regeneration. *J. Physiol.* 594:6753–6765. https://doi.org/10.1113/JP272831

Schonthaler, H.B., J.M. Lampert, A. Isken, O. Rinner, A. Mader, M. Gesemann, V. Oberhauser, M. Golczak, O. Biehlmaier, K. Palczewski, et al. 2007. Evidence for RPE65-independent vision in the cone-dominated zebrafish retina. *Eur. J. Neurosci.* 26:1940–1949. https://doi.org/10.1111/j.1460-9568.2007.05801.x

Schulze, H., C. Michel, and G. van Echten-Deckert. 2000. Dihydroceramide desaturase. *Methods Enzymol.* 311:22–30. https://doi.org/10.1016/S0076-6879(00)11063-8

Seeliger, M.W., C. Grimm, F. Ståhlberg, C. Friedburg, G. Jaissle, E. Zrenner, H. Guo, C.E. Remé, P. Humphries, F. Hofmann, et al. 2001. New views on RPE65 deficiency: the rod system is the source of vision in a mouse model of Leber congenital amaurosis. *Nat. Genet.* 29:70–74. https://doi.org/10.1038/ng712

Sharma, S., S.L. Ball, and N.S. Peachey. 2005. Pharmacological studies of the mouse cone electroretinogram. *Vis. Neurosci.* 22:631–636. https://doi.org/10.1017/S0952523805225129

Shirato, S., H. Maeda, G. Miura, and L.J. Frishman. 2008. Postreceptoral contributions to the light-adapted ERG of mice lacking b-waves. *Exp. Eye Res.* 86:914–928. https://doi.org/10.1016/j.exer.2008.03.008

Sillman, A.J., H. Ito, and T. Tomita. 1969. Studies on the mass receptor potential of the isolated frog retina. I. General properties of the response. *Vision Res.* 9:1435–1442. https://doi.org/10.1016/0042-6989(69)90059-5

Stecher, H., M.H. Gelb, J.C. Saari, and K. Palczewski. 1999. Preferential release of 11-cis-retinol from retinal pigment epithelial cells in the presence of cellular retinaldehyde-binding protein. *J. Biol. Chem.* 274:8577–8585. https://doi.org/10.1074/jbc.274.13.8577

Stubbs, G.W., J.C. Saari, and S. Futterman. 1979. 11-cis-Retinal-binding protein from bovine retina. Isolation and partial characterization. *J. Biol. Chem.* 254:8529–8533.

Takahashi, Y., G. Moiseyev, Y. Chen, O. Nikolaeva, and J.X. Ma. 2011. An alternative isomerohydrolase in the retinal Müller cells of a cone-dominant species. *FEBS J.* 278:2913–2926. https://doi.org/10.1111/j.1742-4658.2011.08216.x

Wang, J.S., and V.J. Kefalov. 2009. An alternative pathway mediates the mouse and human cone visual cycle. *Curr. Biol.* 19:1665–1669. https://doi.org/10.1016/j.cub.2009.07.054

Wang, J.S., and V.J. Kefalov. 2011. The cone-specific visual cycle. *Prog. Retin. Eye Res.* 30:115–128. https://doi.org/10.1016/j.preteyeres.2010.11.001

Wang, J.S., M.E. Estevez, M.C. Cornwall, and V.J. Kefalov. 2009. Intra-retinal visual cycle required for rapid and complete cone dark adaptation. *Nat. Neurosci.* 12:295–302. https://doi.org/10.1038/nn.2258

Wenzel, A., C.E. Reme, T.P. Williams, F. Hafezi, and C. Grimm. 2001. The Rpe65 Leu450Met variation increases retinal resistance against light-induced degeneration by slowing rhodopsin regeneration. *J. Neurosci.* 21:53–58.

Wenzel, A., J. von Lintig, V. Oberhauser, N. Tanimoto, C. Grimm, and M.W. Seeliger. 2007. RPE65 is essential for the function of cone photoreceptors in NRL-deficient mice. *Invest. Ophthalmol. Vis. Sci.* 48:534–542. https://doi.org/10.1167/iovs.06-0652

Wu, J., N.S. Peachey, and A.D. Marmorstein. 2004. Light-evoked responses of the mouse retinal pigment epithelium. *J. Neurophysiol.* 91:1134–1142. https://doi.org/10.1152/jn.00958.2003

Xue, Y., S.Q. Shen, J. Jui, A.C. Rupp, L.C. Byrne, S. Hattar, J.G. Flannery, J.C. Corbo, and V.J. Kefalov. 2015. CRALBP supports the mammalian retinal visual cycle and cone vision. *J. Clin. Invest.* 125:727–738. https://doi.org/10.1172/JCI79651

Zhang, J., Z. Dong, S.R. Mundla, X.E. Hu, W. Seibel, R. Papoian, K. Palczewski, and M. Golczak. 2015a. Expansion of first-in-class drug candidates that sequester toxic all-trans-retinal and prevent light-induced retinal degeneration. *Mol. Pharmacol.* 87:477–491. https://doi.org/10.1124/mol.114.096560

Zhang, J., P.D. Kiser, M. Badiee, G. Palczewska, Z. Dong, M. Golczak, G.P. Tochtrop, and K. Palczewski. 2015b. Molecular pharmacodynamics of emixustat in protection against retinal degeneration. *J. Clin. Invest.* 125:2781–2794. https://doi.org/10.1172/JCI80950

Supplemental material

Kiser et al., https://doi.org/10.1085/jgp.201711815

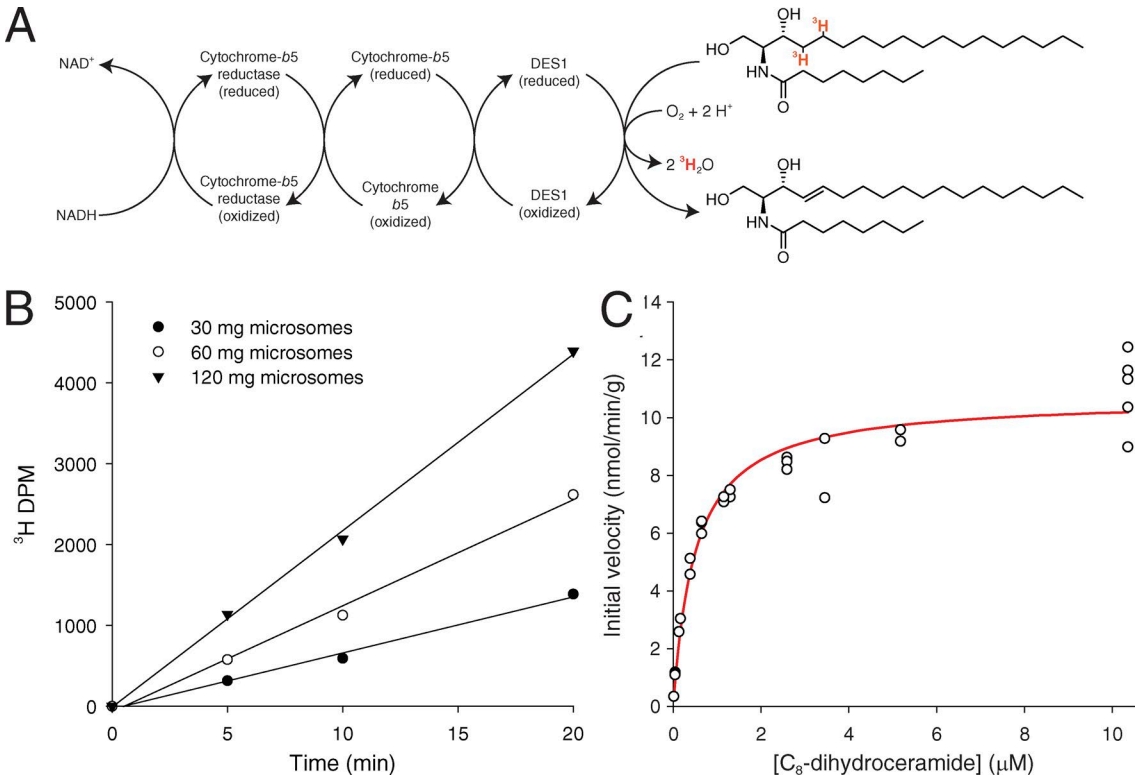

Figure S1. **Schematic and validation of the DES1 activity assay. (A)** DES1 dihydroceramide desaturase activity relies on NADH to provide electrons needed for production of an electrophilic, activated oxygen species that abstracts hydrogen from the substrate. The assay system uses a ^{3}H-4,5–labeled synthetic dihydroceramide as a substrate. DES1 activity specifically releases tritium from the substrate as water, which is separated from unreacted substrate and measured to quantify enzymatic activity. **(B)** Assessment of the linear range of the DES1 activity assay. Reactions were performed at 37°C for 0, 5, 10, and 20 min in the presence of 30, 60, and 120 mg *Lrat*$^{-/-}$ mouse liver microsomes at a fixed substrate concentration of 0.5 μM. Under these conditions, the assay was relatively linear with respect to both time and enzyme concentration. **(C)** Steady-state kinetics of mouse liver DES1 activity toward C_8-dihydroceramide. Assays were performed as described in the Materials and methods section with increasing concentrations of unlabeled C_8-dihydroceramide and a fixed quantity of 4,5-^{3}H-C_8-dihydroceramide. V_{max} and K_m values of 10.7 ± 0.3 nmol/min/g and 0.50 ± 0.07 μM, respectively, were determined for this assay system based on a total number of 28 data points measured in three separate experiments spanning a range of C_8-dihydroceramide concentrations from 0.011 to 10.4 μM.

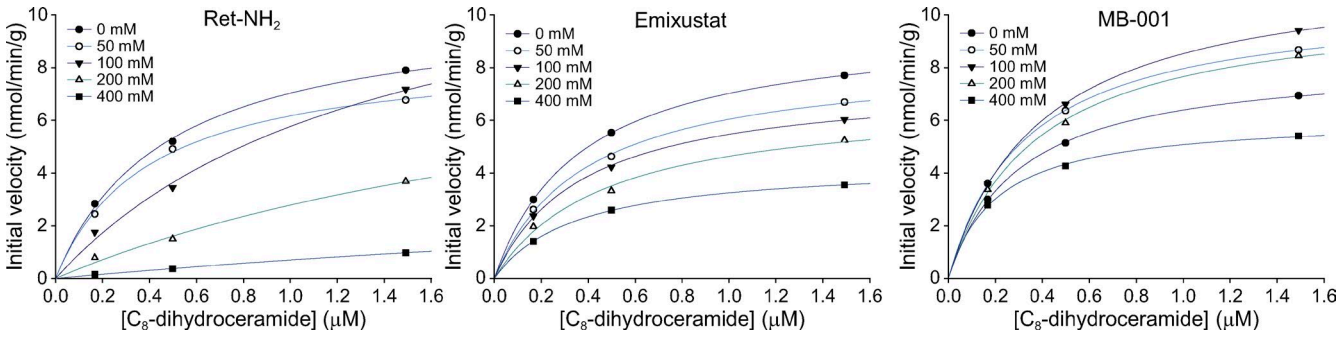

Figure S2. **Effects of RPE65 inhibitors on DES1 enzymatic function.** DES1 dihydroceramide desaturase assays were performed according to the standard method in the presence of the indicated compounds at substrate concentrations below, at, and above the K_m value for C_8-dihydroceramide. The steady-state kinetic constants and the best fit mode of reversible inhibition derived from global curve fitting along with the estimated K_i values are shown in Table S1.

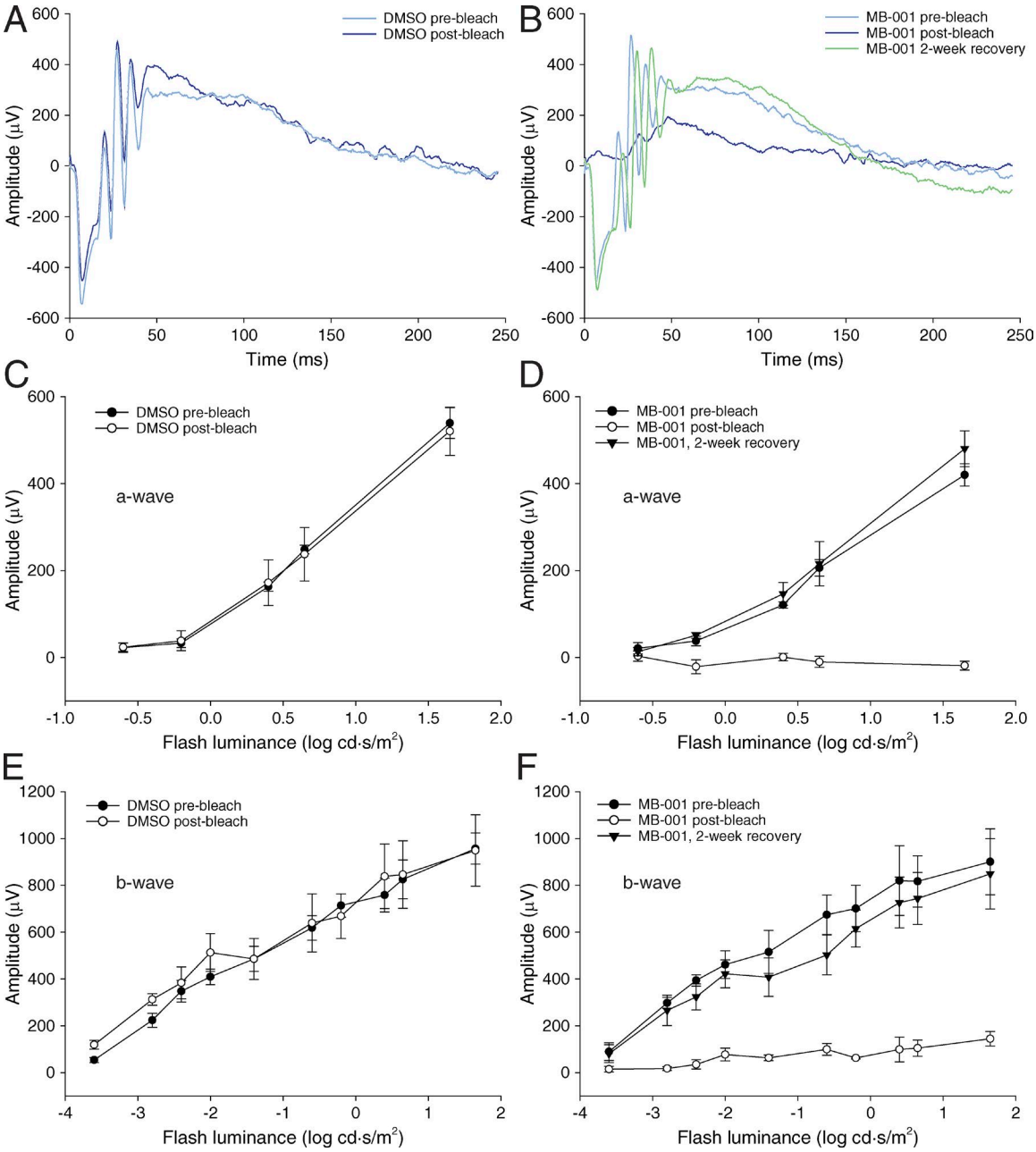

Figure S3. **Effects of MB-001 on dark-adapted mouse ERG responses. (A and B)** ERG responses to a 1.65 log cd·s/m^2 strobe flash recorded from mice (C57BL/6J, 2 mo old) that received IP DMSO vehicle or 8 mg/kg MB-001 immediately before, 22 h after, and 2 wk after a strong photobleach (10 min × 10,000 lux). **(C and D)** Plots of the scotopic a-wave amplitudes for the two groups of mice. **(E and F)** Scotopic b-wave amplitudes for the two groups of mice. DMSO group, n = 4; MB-001 group, n = 3. The data are shown as means ± SEM.

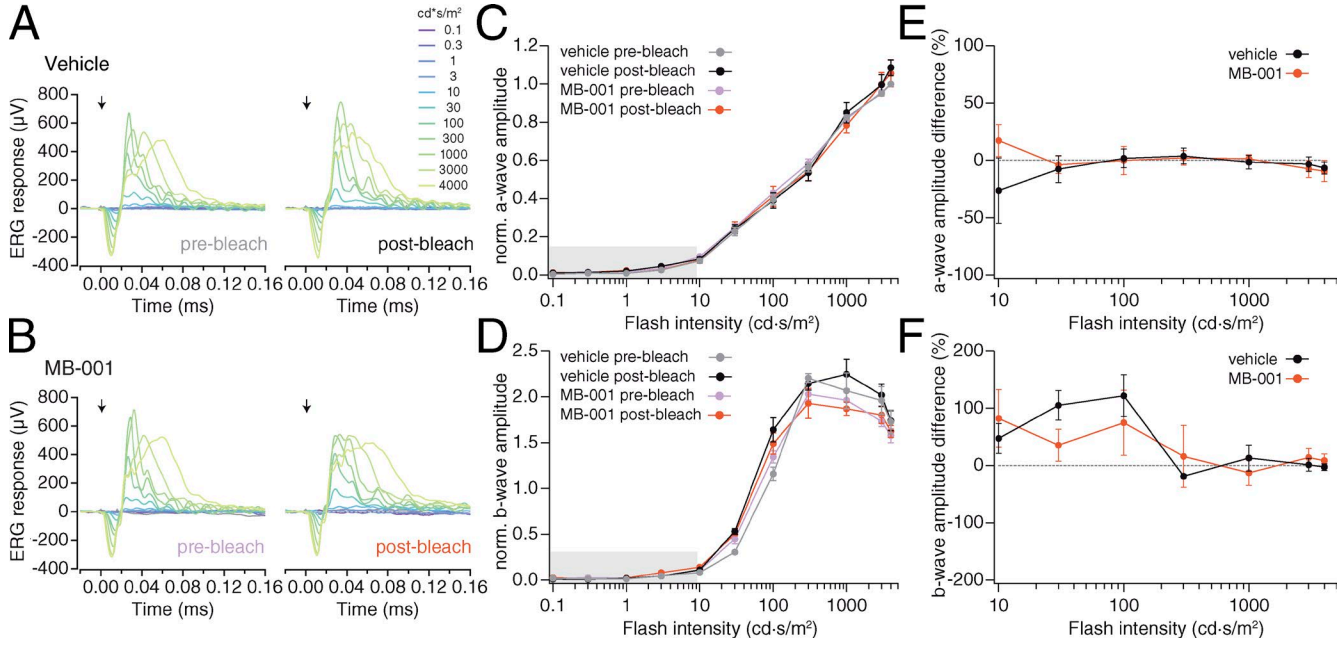

Figure S4. **Impact of MB-001 treatment on ERG responses in ground squirrels after the multiday dosing schedule used in wild-type mice. (A and B)** ERG responses from a single representative ground squirrel after vehicle (A) or MB-001 (B) treatment showing minimal effects of MB-001 treatment on cone function. ERG recordings were made in light-adapted 6-mo-old squirrels after 3 d of vehicle or MB-001 treatment before (left) and 10 min after (right) bleaching (see Materials and methods) using a brief flash of variable intensity as stimulation (black arrows, three to five trials per flash intensity). During the 3 d of treatment, animals were housed in normal cyclical lighting conditions. **(C and D)** Treatment group averages of ERG responses, which do not reveal systematic differences between vehicle- and MB-001–treated animals. We obtained mean a-wave and b-wave amplitudes at each light intensity after normalization by the a-wave amplitude to the 4,000 cd·s/m^2 flash before bleaching. We excluded responses to flash intensities <10 cd·s/m^2 (shaded regions) because they were small and corrupted by noise. **(E and F)** Changes in ERG responses induced by bleaching are not significantly different between treatment groups using this original treatment schedule. We obtained mean a-wave and b-wave amplitude differences (prebleach response − postbleach response; n = 4 squirrels; error bars represent SEM) that show no significant differences at any light intensity between treatments. We compared these ratios as paired measurements (vehicle vs. MB-001) with Wilcoxon rank–sum tests using 5% as the significance level.

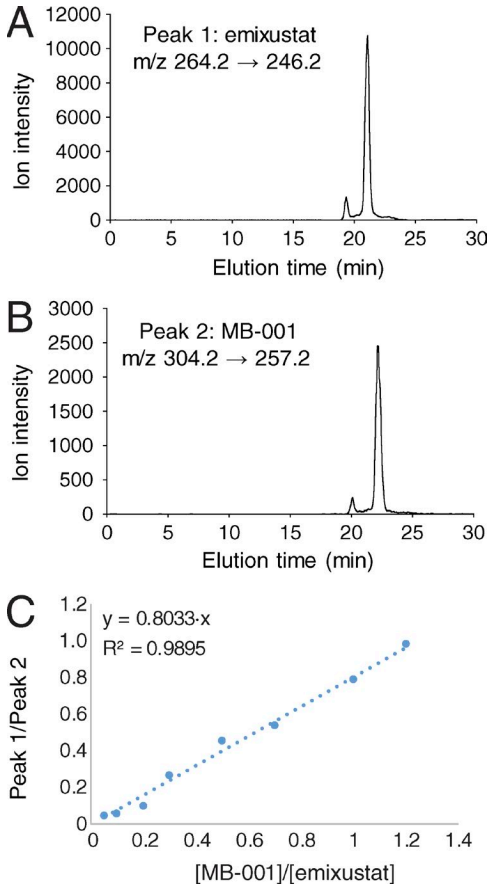

Figure S5. **Standard curve for MB-001 quantification.** 2 nmol emixustat was spiked into a serial solution of MB-001 (0–2.4 nmol) in ethanol. 100 µl of the resulting solutions was injected into a liquid chromatography/mass spectrometry system. **(A and B)** The peak areas of emixustat chromatograms, recorded by selective reaction monitoring at m/z 264.2→246.2 (A) and MB-001 at m/z 304.2→257.2 (B), were recorded. **(C)** A standard curve depicting the ratio of the corresponding peak areas of MB-001 to emixustat and the ratio of their known amounts used in the experiment.

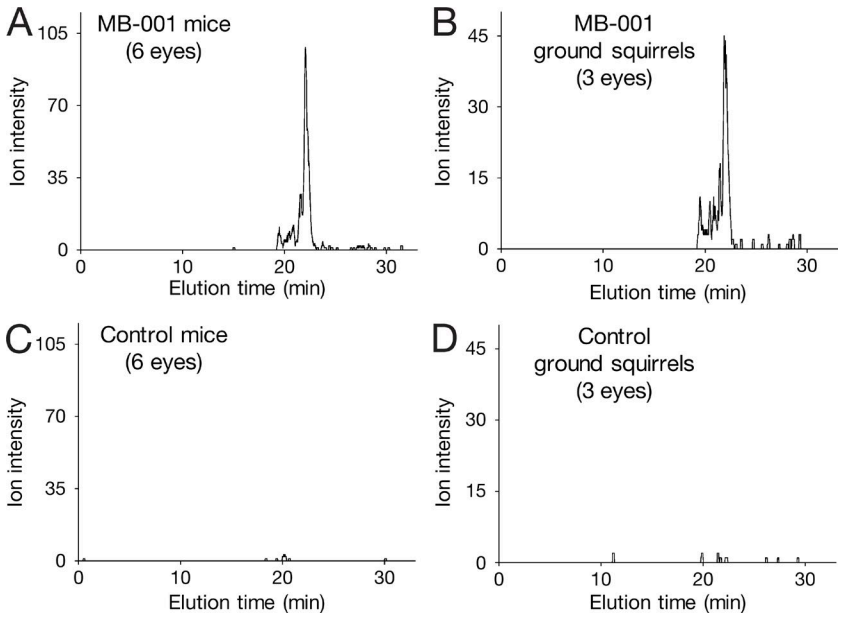

Figure S6. **Quantification of MB-001 levels in mouse and squirrel eyes.** Eye extracts were dissolved in ethanol containing 2 nmol emixustat. 100 µl of the solution was injected into the liquid chromatography/mass spectrometry system. **(A–D)** The chromatogram obtained by selective reaction monitoring at m/z 304.2→257.2 demonstrated that the eyes of C57BL/6J mice (A) and ground squirrels (B) treated with MB-001 both contained substantial amounts of the compound, although the peaks of MB-001 in the eyes from the animals treated with DMSO were negligible (C and D). The amounts of MB-001 in both animals were calculated based on the standard curve shown in Fig. S5.

Table S1. **Steady-state kinetic constants obtained for DES1-mediated dihydroceramide desaturase activity in the presence of RPE65 inhibitors**

Concentration	**Emixustat**		**MB-001**		**Ret-NH$_2$**	
µM	V_{max}	K_m	V_{max}	K_m	V_{max}	K_m
400	4.4	0.35	6.1	0.21	4.9	6.1
200	6.8	0.47	10.5	0.37	10.4	2.7
100	7.5	0.37	11.9	0.39	13.9	1.4
50	8.4	0.38	10.6	0.33	8.6	0.40
0	9.6	0.37	8.3	0.30	10.3	0.47
Mode of inhibition	Noncompetitive; K_i = 360 µM		Noninhibitory		Partial mixed or uncompetitive; K_i = ~80 µM	

V_{max} and K_m values were derived by curve fitting as shown in Fig. S2. The bottom row shows the best fit mode of inhibition and associated K_i values derived from global analysis of the data. The activity simulation and minor inhibition of DES1 activity at higher concentrations precluded global fit analysis for MB-001.